FACULDADE DE ENGENHARIA DA UNIVERSIDADE DO PORTO

Layout Optimization and Power Averaging of an Airborne Wind Energy Farm

Rui Carvalho da Costa

Mestrado em Engenharia Eletrotécnica e de Computadores

Supervisor: Luís Tiago de Freixo Ramos Paiva

Second Supervisor: Luís Augusto Correia Roque

June 30, 2023

Resumo

As energias renováveis são fundamentais para prevenir as alterações climáticas e mitigar as suas consequências mais graves. Para isso, existem inúmeras energias limpas e sustentáveis disponíveis para substituir a procura por combustíveis fósseis, sendo que o vento é uma das fontes de energia renovável mais proeminentes e importantes para produção em grande escala.

Uma tecnologia emergente na área das energias renováveis são os sistemas aéreos de energia eólica, que utiliza *kites* conectados a uma estação no solo por um cabo para produzir energia através do vento a altas altitudes. Os baixos custos de construção e de manutenção, bem como a adaptabilidade da tecnologia, distinguem-na de outras tecnologias convencionais, nomeadamente das turbinas eólicas. Pode ser ainda utilizado um parque eólico usando esta tecnologia, ou seja, um conjunto de unidades para produzir energia em grande escala.

A dissertação aborda o problema de otimização da disposição de unidades, bem como a suavização da onda de potência resultante de um parque que utiliza sistemas aéreos de energia eólica. Além disso, também se discute acerca do número de unidades, a sua localização e regime de operação otimizados para uma área específica. Tendo em conta os múltiplos fatores que o sistema pode apresentar, otimizar este parque para maximizar a produção de energia é um desafio exigente. Um dos principais fatores inclui a distância mínima necessária entre *kites* para evitar colisões, mantendo simultaneamente o objetivo de produção máxima de energia do parque. Para esta maximização, é necessário determinar um equilíbrio entre o número de unidades e a potência máxima que cada uma proporciona, considerando diferentes *layouts* do conjunto das unidades.

Além disso, a flutuação da onda de potência resultante produzida por um parque eólico desta tecnologia é também um problema que afeta a sua integração com a rede elétrica. Para superar este problema, é abordada a sincronização de ciclos de voo das várias unidades em grupos. Para suavizar estas flutuações, também é estudado um determinado desfasamento nos ciclos das unidades entre grupos, permitindo mitigar as flutuações de potência originadas pela natureza cíclica desta tecnologia.

Esses problemas são solucionados através da utilização de um algoritmo de otimização, programado em *MATLAB*. Esta metodologia utiliza um *Biased Random Key Genetic Algorithm*, capaz de encontrar uma solução ótima num tempo de simulação razoável e com um esforço computacional mínimo. São também utilizados dados reais de vento para garantir a validade dos resultados das simulações em cenários reais. Por último, o *wind shear model* foi incorporado no código, fornecendo uma melhor estimativa dos dados de vento, contribuindo para uma solução mais precisa. Assim, o algoritmo está melhor adaptado para ser usado para aplicações do mundo real.

Abstract

Renewable energies are critical to prevent climate change and mitigate its most severe consequences. There are numerous clean and sustainable energies available to replace the demand for fossil fuels. Wind is one of the most prominent and important renewable energy sources for large-scale production.

One emerging technology in the renewable energy area is the Airborne Wind Energy Systems (AWES), which harness wind in higher altitudes through kites connected to a ground station to produce electricity. The low construction and maintenance costs and adaptability of AWES technology distinguish it from other conventional technologies such as wind turbines. For this, a kite farm might be utilised, which is a set of single units gathered to produce energy on a large scale.

The dissertation addresses the layout optimization problem of a set of single units, as well as the smoothing and averaging of the resultant power in a wind farm using AWES, detailing the number of units, their location, and operation regime in a given area. Considering the multiple factors that the system might has, optimizing this farm to generate the maximum power output for the given area is a demanding task. One of the main factors include the minimum distance between kites required to avoid collisions while ensuring the maximum power production of the farm. To maximize farm production, a trade-off between the number of units and the maximum power each one provides is required and different layouts are considered.

Furthermore, the fluctuation of the power output of a kite farm is also a problem that affects its integration into the electrical grid. To overcome this, flight synchronisation of the producing units are addressed. In order to smooth the fluctuations of the resultant power waveform, the operation of the cycles of the units of the farm is addressed, with the study of a certain phase shift between groups, enabling to mitigate the power fluctuations originated by the cyclic nature of this technology.

These problems are addressed by using an optimization algorithm, coded in MATLAB. This methodology consists of a Biased Random Key Genetic Algorithm (BRKGA), capable of finding an optimal solution in a reasonable simulation time and with minimal computational effort. Real wind data is studied to ensure the validity of the results in practical scenarios. Moreover, the incorporation of the wind shear model provides an improved estimation of wind data, to further apply the algorithm to real-world applications.

Acknowledgements

The elaboration of a thesis is described as a solitary activity, but this description does not apply to my experience, as I had a lot of company and collaboration. With this, I would like to thank to...

My supervisors Professor Luis Tiago Paiva and Professor Luis Roque. I thank them for all the guidance and development opportunity to work in this so emerging and interesting area. Their help was indispensable to the completion of this work. And Manuel Fernandes, who has always been available and willing to help whenever I needed it.

Everyone involved in the UPWIND Project. Their collective support and companionship throughout these months have been crucial to the success of my work.

My family, namely my parents and sister. I appreciate the support and encouragement throughout my education, especially during this cycle.

My friends. Their presence, entertainment, and support have made this entire journey a truly enjoyable experience. I am thankful for their friendship and for the fun times we have shared.

Finally, I want to thank the financial support by national funds through the FCT/MCTES (PIDDAC) under Projects KEFCODE-KiteFarms 2022.02320.PTDC, UPWind-ATOL 2022.02801.PTDC, SYSTEC–Research Center for Systems and Technologies (Base-UIDB/00147/2020 and Programmatic UIDP/00147/2020 funds), ARISE - Associate Laboratory Advanced Production and Intelligent Systems (LA/P/0112/2020).

Rui Carvalho da Costa

"A kite can't really fly free, that's just an expression.
In order to soar high in the sky the string of a kite needs to be anchored.
If the string breaks the kite drops back to the ground.
The kite's freedom depends on it not being as free as he thinks it is."

Simon Napier-Bell

Contents

List of Figures

List of Tables

Abbreviations and Symbols

ACO	Ant Colony Optimization
ACP	Average Cycle Power (W)
AEP	Annual Energy Production (MWh)
A_{Land}	area of the land (m)
AWE	Airborne Wind Energy
AWES	Airborne Wind Energy Systems
BESS	Battery Energy Storage Systems
BRKGA	Biased Random Key Genetic Algorithm
CF	Capacity Factor
ΔP	Deviation of Power (W)
EA	Evolutionary Algorithm
ESS	Energy Storage Systems
Fly-Gen	Flying-Generation
GA	Genetic Algorithms
GHG	Greenhouse Gas
Ground-Gen	Ground-Generation
Hours_{eq}	Equivalent Hours (h)
LCOE	Levelized Cost of Energy
L_{Land}, W_{Land}	length, width of the land (m)
PD	Power Density $\left(\text{W m}^{-2}\right)$
PKS	Pumping Kite Systems
PSO	Particle Swarm Optimization
NDC	Nationally Determined Conditions
R&D	Research and Development
RKGA	Random Key Genetic Algorithm
SA	Simulated Annealing
UNFCCC	United Nations Framework Convention on Climate Change
p	population
p_e	elite population
ρ_e	percentage of elite population
ρ_{cross}	percentage of population from crossover
p_{nkeys}	new keys population
ρ_{nkeys}	percentage of new keys population
ρ_a	crossover parameter
h	height (m)
z_0	terrain roughness
P_{avg}	kite wind farm average power (kW)
P_{nom}	nominal power (W)

$P_{\min}, P_{\max}$	minimum and maximum power (kW)
(x, y, z)	Cartesian coordinates
(r, φ, β)	spherical coordinates
r	radial distance (m)
φ	azimuth angle (rad)
β	elevation angle (°)
τ	tangential plane
σ	instant position in the tangential plane (rad)
$\Delta\beta$	deviation of elevation angle (°)
$\beta_{\min}, \beta_{\max}$	minimum and maximum elevation angles (°)
β_{re}	elevation angle during retraction phase (°)
β_{in}	elevation angle for the retraction inside flight envelope (°)
β_{out}	elevation angle for the retraction out of flight envelope (°)
$\Delta\varphi$	deviation of azimuth angle (rad)
$\vec{v}_w$	wind velocity $\left(\mathrm{m\,s^{-1}}\right)$
$\vec{v}_k$	kite velocity $\left(\mathrm{m\,s^{-1}}\right)$
$\vec{v}_{k,r}$, $\vec{v}_{k,\tau}$	radial, tangential component of kite velocity $\left(\mathrm{m\,s^{-1}}\right)$
$\vec{v}_a$	apparent wind velocity $\left(\mathrm{m\,s^{-1}}\right)$
$\vec{v}_{a,r}$, $\vec{v}_{a,\tau}$	radial, tangential component of apparent wind velocity $\left(\mathrm{m\,s^{-1}}\right)$
f	kite radial speed and wind speed ratio
λ	kite tangential speed and wind speed ratio
α	angle of attack (°)
$\vec{\mathrm{F}}^{\mathrm{lift}}$	lift force (N)
$\vec{\mathrm{F}}^{\mathrm{lift}}_{\mathrm{turning}}$	turning lift (N)
$\vec{\mathrm{F}}^{\mathrm{drag}}$	drag force (N)
c_L	aerodynamic lift coefficient
$c_{L,r}$	radial component of the lift force coefficient
c_D	aerodynamic drag coefficient
c_R	aerodynamic force coefficient
R	radius of circular trajectory (m)
ψ	roll angle (rad)
$\psi_{\max}$	maximum roll angle (rad)
a_{turning}	lateral acceleration $\left(\mathrm{m\,s^{-2}}\right)$
$a_{\mathrm{centripetal}}$	centripetal acceleration $\left(\mathrm{m\,s^{-2}}\right)$
$\mathrm{F_T}$	instantaneous traction force (N)
P_T	instantaneous power during traction phase (W)
P_{tr}	average power during traction phase (W)
P_{re}	average power during retraction phase (W)
ρ	air density $\left(\mathrm{kg\,m^{-3}}\right)$
A	wing reference area of kite $\left(\mathrm{m^2}\right)$
m	kite mass (kg)
$r_{\min}, r_{\max}$	minimum, maximum tether length constraints (m)
$L_{\min}, L_{\max}$	minimum, maximum tether length (m)
z_{max}	maximum kite altitude (m)
P_c	average cycle power (W)
η_{tr}	efficiency of converting mechanical to electrical Power
η_{re}	efficiency of converting electrical to mechanical Power
E_{tr}	energy produced during traction phase (W s)

E_{re}	energy consumed during retraction phase $(\mathrm{W\,s})$
t_{tr}	time during traction phase (s)
t_{re}	time during retraction phase(s)
t_{tran}	time during transition phase (s)
d_1	aligned distance between units according to the wind direction (m)
d_2	perpendicular distance between units according to the wind direction (m)
d_3	distance to the border (m)
N_{kites}	number of kites
n_{sq}	number of kites in a squared layout
n_{hex}	number of kites in a hexagonal layout
T_c	cycle time (s)
Θ	phase shift (s)

Chapter 1

Introduction

Wind energy plays a vital role as a renewable energy source, holding significant potential for reducing greenhouse gas (GHG) emissions and mitigating the impacts of climate change. As of 2019, wind energy accounted for 5% of global electricity generation [9].

Conventionally, wind turbine systems have focused on harnessing surface-level winds, which tend to be less predictable and weaker compared to winds at higher altitudes [10]. However, recent advancements in wind energy technology have prompted the exploration of alternative approaches, including AWES. By using aircrafts connected by a tether to the lighter and less robust infrastructures, AWES enable operations at higher altitudes, where winds are stronger and more consistent. Thus, this presents an opportunity to enhance energy generation efficiency and cost-effectiveness.

The optimization and design of AWES are active areas of research due to the multitude of factors influencing their performance. Among these factors, the configuration of single units within the kite wind farm plays a pivotal role in determining energy output, guaranteeing a better connection to the electrical grid.

Addressing the challenges associated with AWES farm design is crucial for maximizing efficiency and ensuring the viability of this technology. By gaining a comprehensive understanding of the factors influencing system performance, it becomes possible to design configurations that effectively harness wind energy. This research aims to investigate the difficulties encountered in wind farms, with a particular focus on layout optimization of the wind farm, as well as power deviations and the importance of achieving an averaged power output to facilitate grid integration. The research approach entails utilising computational simulations and optimization algorithms to evaluate the performance of the wind farm based on the arrangement of units within a given terrain and their operational settings. The specific objectives of this research are as follows:

1. The development of a computational algorithm capable of optimizing power output for individual units within an AWES. This algorithm will include optimization methods, such as genetic algorithms, to determine the optimal configuration of AWES units based on the identified critical factors taking into account interactions between units, wind dynamics, and operational constraints.

2. The identification of key factors influencing the efficiency of AWES, with a specific emphasis on achieving power output smoothing and averaging within wind farms. By analysing the impact of these factors, the research will provide insights into how to optimize the arrangement of AWES units to improve the overall performance of the system.

3. The validation of algorithm accuracy using real data from existing measurement installations. The results will serve to validate the effectiveness of the computational algorithm and provide practical insights into its performance under real operating conditions.

Chapter 2 of this thesis provides an overview of climate change and highlights the role of the energy sector in addressing this global issue. The chapter explores the escalating energy demand, the significance of fossil fuels, and the initiatives undertaken by the United Nations Framework Convention on Climate Change (UNFCCC) and the Paris Agreement to effectively combat these challenges. It also sets the context for the research by emphasising the urgency and importance of transitioning to sustainable energy sources, including wind power.

Chapter 3 delves deeply into the fundamental aspects of wind energy and AWES, offering a comprehensive exploration of the technology and its vast potential. The chapter examines the working principles of AWES and studies existing innovations and principles that have emerged in this field, which demonstrates a solid understanding of the capabilities and possibilities of AWES technology.

Chapter 4 is dedicated to formulating the fundamental principles that govern the operation of kite wind farms, with a specific emphasis on wind forecast and study, as well as the behaviour of individual units in relation to wind dynamics and measurements that enable the evaluation of the performance of the wind farm. This chapter thoroughly explores the interactions between the various components of a single unit within a wind farm, namely the aircraft, tethers, and the influence of the wind. By analysing these interactions, the chapter serves as the basis for developing the computational algorithm to optimize power output.

Chapter 5 provides a comprehensive overview of the different components involved in designing a kite wind farm. The chapter digs into the complexities of AWES farm design, discussing essential factors such as grid integration challenges, optimal unit spacing, and considerations for different layouts. By addressing these critical aspects, the chapter provides various proposals for the development of efficient and effective AWE farms.

Chapter 6 outlines the methodology employed, providing insights into the computational simulations and optimization algorithms utilised to evaluate wind farm performance. The chapter describes the application of Biased Random Key Genetic Algorithms (BRKGA) and its application for this problem resolution.

In Chapter 7, the thesis presents the results obtained from a case study with real-world data, showcasing the practical implementation and performance of the developed computational algorithm. The chapter highlights the analysis conducted during the study, including assessments of diverse layouts and power output smoothing.

Finally, Chapter 8 draws conclusions based on the research findings and proposes potential directions for future work in the field of AWES technology. The chapter discusses the contributions of the research in advancing AWES and emphasises the importance of the implementation of this efficient and sustainable type of technology for a greener future.

By addressing the aforementioned objectives, this research strives to contribute to the advancement of this type of technology, facilitating the efficient and sustainable harnessing of wind energy.

Chapter 2

Climate Change

This chapter addresses the global challenge of climate change and its implications. It discusses the increasing energy demand driven by economic development, the dominant role of fossil fuels, and the need for a transition to cleaner and sustainable energy sources.

The chapter also highlights international efforts, such as the UNFCCC and the Paris Agreement, aimed at reducing emissions and promoting renewable energy adoption to shape a low-carbon future.

2.1 Rise of Energy Demand

The global demand for energy has increased over time due to a variety of factors, as seen in Figure 2.1, such as population growth, economic development, and urbanisation. This increase almost reaches 1% per year [11]. As society becomes more urbanised, there is a necessity for energy to power housing, businesses and transportation. There are other factors that contribute to the rising demand for energy, including technological advances, like the increasing use of electronic devices and the expansion of infrastructure. Meeting this growing need for energy poses challenges, including finding ways to generate and distribute energy efficiently and sustainably [11]. It also requires balancing the need for energy with concerns about the environmental and social impacts of energy production and use.

2.2 Fossil Fuels

Fossil fuels, such as coal, oil, and natural gas, have long been used to generate energy on a large scale. These fuels are formed over millions of years from the remains of plants and animals, and contain a large amount of stored energy in the form of chemical bonds. When fossil fuels are burned, this stored energy is released, providing a source of heat and power.

Fossil fuels are attractive as an energy source because they are abundant, relatively cheap, and convenient to transport and store. They are also relatively easy to use to generate energy, which

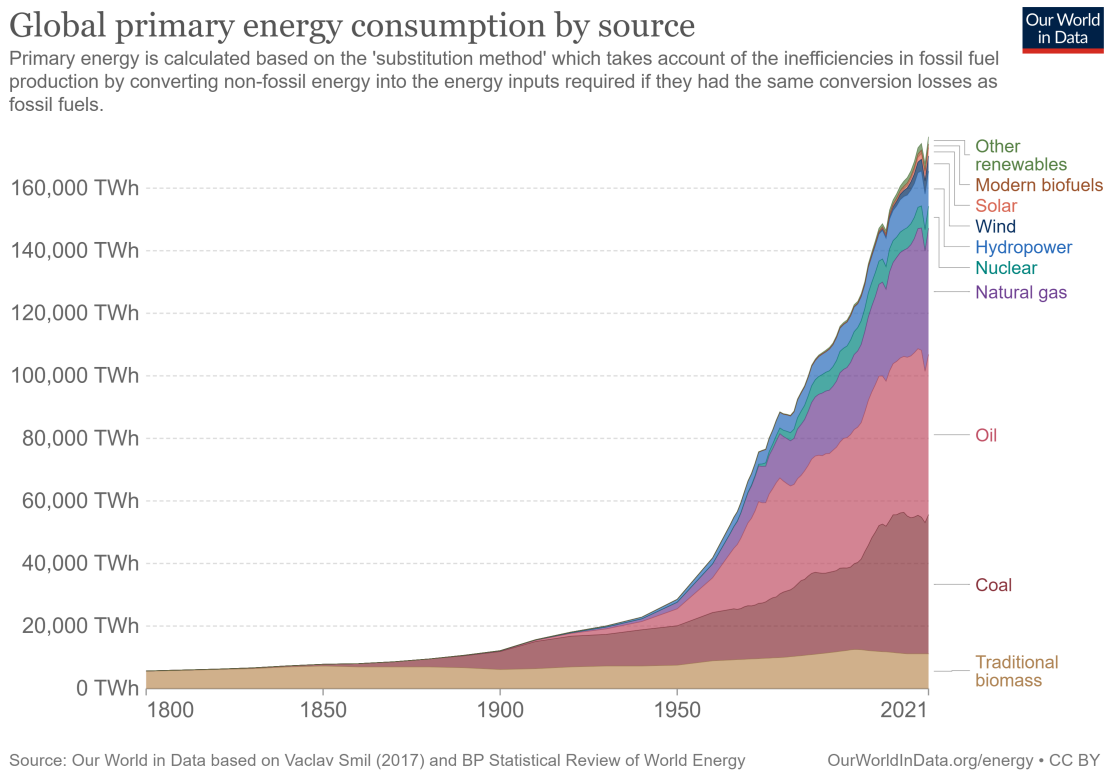

Figure 2.1: Rise of global energy demand [1]

has made them the dominant source worldwide, being responsible for 81% of the primary energy demand [12].

However, the use of fossil fuels to generate energy has significant environmental and social impacts. The burning of fossil fuels releases greenhouse gases (GHG), such as carbon dioxide, into the atmosphere, contributing to climate change. The extraction, transportation, and use of fossil fuels can also negatively impact air and water quality, and the health and well-being of communities.

2.3 Energy Sector

The energy sector is a significant contributor to global warming, as the burning of fossil fuels such as coal, oil, and natural gas releases GHG, such as carbon dioxide, into the atmosphere. These gases trap heat from the sun, causing the average surface temperature of the Earth to rise, a process known as the greenhouse effect. The burning of fossil fuels is the primary source of human-caused GHG emissions, and the energy sector is responsible for almost 3/4 of total greenhouse emissions [2], as seen in Figure 2.2.

To address the problem of global warming, it is necessary to reduce GHG emissions from the energy sector. This can be achieved through a variety of means, including increasing the use of renewable energy sources, such as solar and wind power, and improving energy efficiency. It

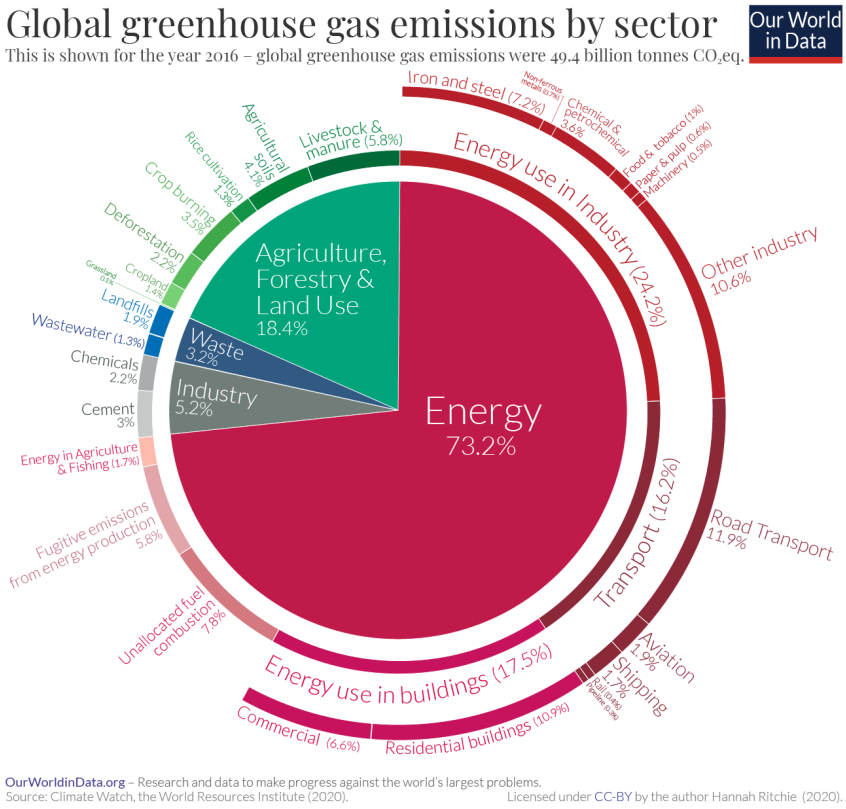

Figure 2.2: Role of energy sector in GHG emissions [2]

may also involve phasing out the use of fossil fuels and transitioning to cleaner, more sustainable energy sources.

Reducing GHG emissions from the energy sector will require significant changes to the way energy is produced, distributed, and consumed. It will also require the development and deployment of new technologies, as well as policy changes at the national and international levels. While the transition to a low-carbon energy system will be challenging, it is necessary to address the problem of global warming and ensure a sustainable future for all.

2.4 UNFCCC and Paris Agreement

To tackle the problem of climate change, the UNFCCC was created in 1992 [13]. The UNFCCC is an international treaty that aims to stop the evolution of climate change by stabilising GHG concentrations in the atmosphere. The treaty establishes a framework for international cooperation to mitigate and adapt to climate change, and it has been ratified by nearly all countries in the world.

One of the key outcomes of the UNFCCC was the adoption of the Paris Agreement in 2015. The Paris Agreement is a legally binding treaty that aims to limit global warming to well below $2°C$ above pre-industrial levels, with the goal of limiting warming to $1.5°C$ if possible [14].

The Paris Agreement establishes a framework for countries to develop and submit voluntary plans, known as Nationally Determined Contributions (NDC), outlining their efforts to reduce gas

emissions and adapt to climate change. The agreement also establishes a financial mechanism to help developing countries transition to low-carbon economies and adapt to the impacts of climate change [13].

The UNFCCC and the Paris Agreement are critical instruments in the global effort to address climate change and protect the planet for future generations. Besides this, it is also extremely important to mention that the project aligns with the principles outlined in [15]. Specifically, it aims to support Goal 7: Affordable and Clean Energy and Goal 13: Climate Action, which fall under the category of Sustainable Development.

Chapter 3

Fundamental Aspects

In this chapter, we delve into the fundamental aspects of wind energy and AWES. These aspects provide a solid foundation for understanding the different principles and operations of AWES, as well as the various types of systems.

The first section of this chapter focuses on wind energy, which serves as the primary source harnessed by AWES. Here, we explore the potential of wind energy as a clean and renewable source of power, highlighting its environmental benefits and global significance in addressing energy challenges and the importance of understanding the fundamentals of wind energy for comprehending the role of AWES in harnessing this abundant resource.

Moving on to the core of this chapter, we dive into AWES state of the art. We explore different approaches to AWES, including ground-generation (Ground-Gen) systems and flying-generation (Fly-Gen) systems. We discuss the principles, advantages, and challenges associated with each approach, showing the diverse possibilities and advancements in AWES technology.

Within the realm of AWES, we explore various aspects related to flight operations, wing types used in crosswind systems, and different methods of take-off and landing. These aspects play a crucial role in the design, operation, and efficiency of AWES. Furthermore, we highlight notable projects in the field of AWES, showcasing real-world applications and advancements in this emerging sector.

We touch upon the concept of kite wind farms, which involve the deployment of multiple AWES units in a coordinated manner to generate electricity at a larger scale. Besides that, we also discuss the benefits and considerations associated with kite wind farms, providing insights into the potential of integrating AWES into existing wind energy infrastructure.

Lastly, by exploring the working principles and various aspects of AWES, this chapter sets the stage for a deeper understanding of the technology, its applications, and its role in the future of sustainable energy. Subsequent chapters will further dig into specific aspects of AWES design, operation, and optimization, building upon the foundational knowledge established here.

3.1 Wind Energy

Wind power is only one of several environmentally friendly and renewable energy sources, and it is one of the most fundamental for large-scale energy production. It is a renewable source of electricity that is generated by the movement of air masses.

Wind turbines are devices designed to capture this wind energy and convert it into electricity. The tower, the blades, and the nacelle, which houses the electric generator, gearbox, and control systems, are their essential parts. Wind turbines work by using large blades to harness the energy of the wind [16]. As the wind blows, it turns the blades, which are connected to the rotor. Inside the nacelle, the rotor is connected to a generator, which converts the mechanical energy from the rotor into electrical energy.

Wind turbines are the traditional choice for harnessing wind energy, both on and offshore, because they are relatively simple, reliable, and economical. However, they also have limitations and constraints that can impact their performance and efficiency.

Nowadays, the extraction of wind energy is mostly made by conventional wind turbines, which operate at a relatively low altitude. Higher altitudes have a stronger wind, which means that there is a significant proportion of the kinetic energy available at levels wind turbines do not reach.

Despite the potential advantages of using high-altitude wind energy, doing so with conventional technology would be very difficult since stronger, higher towers and sturdy foundations are required, and these mechanical efforts are not only technically challenging but also expensive [7].

Besides, in order to function effectively, wind turbines require a specified range of wind directions and speeds, as well as a relatively significant quantity of space for their installation. This can limit the availability of suitable sites for wind turbine farms, particularly in urban or densely populated areas.

At last, installing and maintaining wind turbines can be costly, with very high upfront costs, mainly if they are situated in remote or difficult-to-access areas. This can make it challenging for some countries or regions to use wind energy as a reliable source of power.

To address the limitations of traditional wind turbines, an emerging type of wind energy system called AWES has been developed. AWES harness wind energy using airborne devices in high altitudes connected by a tether to the ground station.

AWES offer several advantages. They have the potential to generate more power with fewer single units due to their ability to operate at higher altitudes. They also offer greater flexibility in terms of deployment, as they do not require the same amount of space or infrastructure as ground-based wind turbines [17].

In fact, this concept involves significantly less material cost per unit of usable power compared to other renewable energy sources, resulting in a 90% saving compared to traditional wind turbines [18].

Overall, AWES represent a promising new approach to harnessing wind energy, and they offer the potential to overcome some of the limitations and constraints of traditional wind turbines.

However, it is important to note that AWES are still in the early stages of development and have yet to be widely deployed.

3.2 Airborne Wind Energy Systems

The concept of AWE devices originated in the 1970s, but it is only in recent years that the necessary elements and control technologies have become available [3]. Over the past four decades, the AWE sector has transitioned from conceptual ideas and initial small-scale trials to the development of a diverse range of technology demonstrations. Still, it is in the last decade that the progress in the field has been remarkable.

To illustrate the global research and development (R&D) landscape in the AWE field, Figure 3.1 provides an overview of companies and institutions holding technological advancements and research activities across different regions [3].

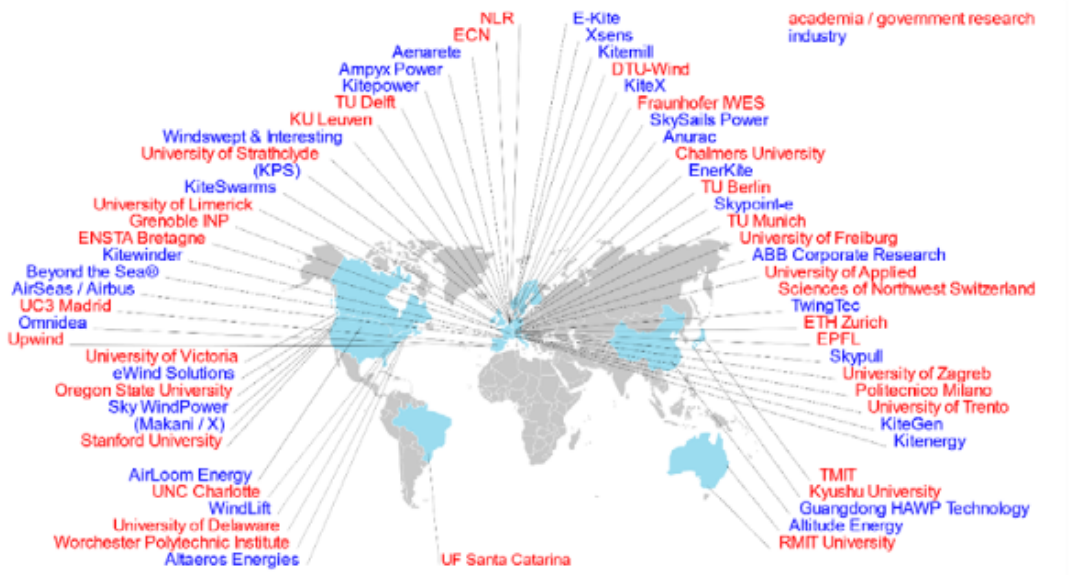

Figure 3.1: Global R&D landscape [3].

AWES typically consist of two primary parts: a ground system and at least one aircraft, which are connected by a tether [19]. From the numerous AWES concepts, we may define Ground-Gen systems, which convert mechanical energy into electrical energy on the ground, and Fly-Gen systems, which generate electricity onboard the aircraft [20].

Each approach has its own advantages and considerations, and ongoing research aims to optimize its performance and efficiency.

3.2.1 Ground-Generation

In Ground-Gen AWES, the motion of an electrical generator is created on the ground through mechanical work performed by traction force that is transferred from the kite to the ground system by a tether.

There are two types of Ground-Gen AWES: those with a fixed ground station and those with a moving ground station, which has a ground station that operates as a moving vehicle. [19].

3.2.1.1 Fixed Ground Station

Fixed Ground-Gen AWES, extensively studied by both private companies and academic research groups, have shown promising potential [21]. One example of such a system is the Pumping Kite System (PKS), which operates on a two-phase cycle.

During the generating phase, the aircraft is flown, generating lift force and traction on the tethers. The traction force drives the rotation of motor-generators connected to winches, producing electricity. In the recovery phase, the motors rewind the tethers, bringing the aircraft back to its starting position at a lower altitude [19].

Fixed ground stations require control systems to optimize energy production and minimize energy consumption during the different phases. However, due to the two-phase cycle, these systems exhibit highly intermittent power output.

3.2.1.2 Moving Ground Station

Moving-ground-station (Ground-Gen) AWES are more complex than fixed-ground-station systems and aim to provide a more constant flow of power, making them easier to connect to the grid [19].

Unlike PKS, the winding and unwinding of ropes in moving-ground-station systems does not significantly affect power production or consumption, and is only used to control the trajectory of the aircraft. In these systems, the generation of electricity occurs through the traction force of the tethers, which drives the rotation or linear motion of a generator using the movement of the ground station rather than the winding mechanism of the tethers.

3.2.2 Flying-Generation

In Fly-Gen, AWES use onboard turbine-generator units that are attached to an airframe and, generally, fly in figure eight or circular crosswind patterns. Then, the electricity generated by these systems is produced onboard the aircraft and transmitted to the ground station via a tether in the tether [3].

This type of generation provides steadier power output, requiring energy only during take-off or landing, and eliminating a two-phased cycle. However, difficulties with the weight growth of the aircraft and the need to send electrical energy to the ground without a stable structure make power generation challenging [7].

3.2.3 Flight Operations

AWES can also be categorised by the path of flight [3]:

1. Crosswind flight, first described by Loyd [22], involves flying in a direction that is perpendicular to the wind flow. This can be achieved through various patterns, including figure of eights or circles. The figure eight pattern is often preferred because it avoids tether twisting, while also allowing for an increase in the relative velocity of the flying wing.

2. AWES that do not involve crosswind flight can be divided into two categories based on the flight pattern and configuration of the aircraft. The first category includes systems that operate in a fully rotating mode (with a circular flight path) or that generate electricity using rotorcraft. The second category includes systems that use the buoyancy flying principle, which involves lifting the aircraft with lighter-than-air gases [17].

As evidenced by the numerous companies and research groups engaged in this area, crosswind flight is the AWES operation that is most frequently used. This is because AWE concepts that make use of crosswind power have a distinct advantage over non-crosswind concepts in terms of the amount of available power, and consequently, the overall economic viability of the system [19].

3.2.4 Wing Types for Crosswind Systems

Crosswind AWES must feature a flying wing that withstand strong traction forces to maintain altitude. Additionally, it should be able to tolerate poor weather and mechanical wear. The design process will require some trade-offs, since these needs usually conflict with one another. The two most common forms of wings are soft and fixed wings [17].

1. Soft wings have many industrial applications. They are suitable for use in AWES due to their compact design, light weight, reliable flight characteristics, and low production costs. Due to their fabric design, they are far more crash-resistant than fixed wings [20]. However, they rely on line steering devices for control, which can be problematic during the recovery phase of the generating cycle [17].

   The lifespan of soft wings is limited by the use of textile materials, so it is important to use the right material to increase durability. High-tensile fibre fabrics are a great option since they are thin and can extend the life of the wings [17].

2. Fixed wings can be used for both Ground-Gen and Fly-Gen. Fixed wings outperform soft wings in terms of aerodynamics due to their high aspect ratio and ability to maintain shape during flight. These wings can withstand high aerodynamic loads and are typically made of carbon or glass fibre composites to support the additional weight of on-board generators[17]. These materials are more expensive and denser than fabric, but they have excellent strength-to-weight ratios and mechanical wear resistance. Fixed wings outlast soft wings, but they

are more expensive to produce and have a higher system mass, limiting their performance at low wind speeds [17]. Another disadvantage is the damage concern in case of a crash [20].

3.2.5 Types of Take-off and Landing for Crosswind Systems

The ability to successfully take off and land is critical to a good operation of an AWES. As such, it is important to understand the various concepts and approaches that have been developed. Currently, there are several options to choose from depending on the type of wing being used [17]. The take-off and landing procedures are very important in the operation of AWES single units to guarantee the safety of the units in case of emergency, such as the case of a lack of wind or excessively high speeds.

3.2.5.1 Take-off and Landing using Soft Wings

There are two approaches for launching soft wings: passive and active.

1. Passive techniques use an arm to elevate the kite to a height where there is sufficient wind speed to create lift force on the kites [17].

2. Active approaches involve the use of additional airborne mass, such as propellers on the control pod, to lift the kite to operational altitudes. These methods have not been implemented due to added power consumption and costs. The landing process for soft wings involves reeling-in the tether with minimal energy consumption [17].

The potential benefits of using a tower in an AWES are being explored, including the ability to lower the elevation angle of the wing, reduce tether mass and drag, and facilitate take-off and landing. However, increased demand for materials, complexity of the system and construction costs and maintenance are some of the disadvantages to consider when building a tower [17].

3.2.5.2 Take-off and Landing using Fixed Wings

The take-off and landing techniques for fixed wings can vary in three main concepts.

1. Linear Horizontal take-off and landing: In this technique, the aircraft is accelerated using an external source, such as a winch or a catapult technology, on a runway with predetermined routes [23]. To maintain forward momentum throughout the rise to the operating height, the aircraft may be equipped with onboard propellers. In order to line the aircraft with the rails for landing, the tether is managed, and braking systems may be required to slow the aircraft down [17].

2. Linear vertical take-off and landing: In this method, the aircraft has internal propellers that, like those on a quadcopter, provide enough thrust for vertical take-off [23]. A reliable controller is necessary for the platform in order to ensure a stable take-off. If the aircraft has a tailplane configuration, this method might not be capable of withstanding high wind

speeds. When the aircraft reaches the operational altitude, a transition phase begins to reset its normal orientation [17].

3. Rotational take-off and landing: For aircraft with fixed wings, the aircraft is attached to the end of a rotating arm and turned to produce centrifugal forces that cause the aircraft to fly in a helical pattern. When the required height is achieved, the rotation is slowed until it ends. In order to connect the aircraft to the rotating arm upon landing, the procedure is reversed, and the tether is reeled-in [17].

3.2.6 Projects in AWES

Although all AWES share a common category, there are numerous relevant companies within this field that utilise and develop different types of technologies. These distinctions can include various elements, such as wing rigidity, flight control techniques, and take-off and landing procedures.

To provide a comprehensive overview of the diverse landscape within the AWES field, Figure 3.2 visually illustrates the different configurations and technologies employed by various companies. This visual representation enhances the understanding of the wide range of approaches and solutions found within the AWES industry.

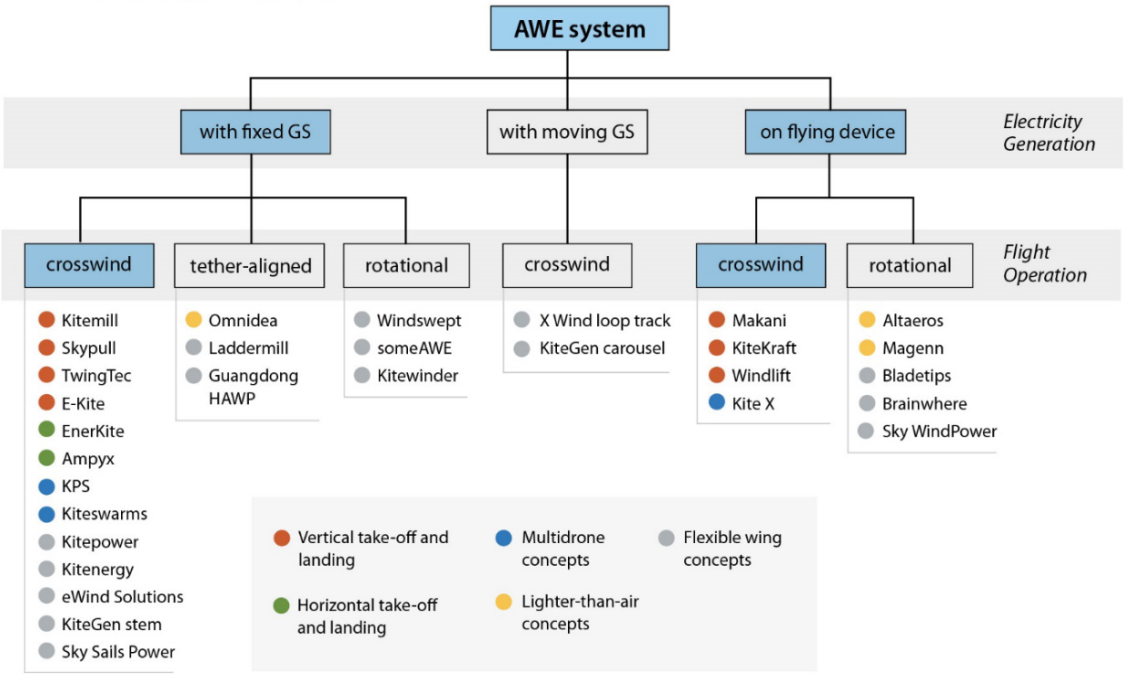

Figure 3.2: Classification of AWES, with list of institutions and developed prototypes [3].

Makani Technologies, in Figure 3.3(a), a company founded in 2006, later acquired by Google, made significant advancements in the field of airborne wind energy [24]. They developed a kite system consisting of a 30-meter carbon fibre wing tethered to wind turbines. This innovative technology allowed the kite to reach altitudes of up to 600 meters and generate a substantial power output of 600 kW [25].

SkySails, in Figure 3.3(b), a Hamburg-based company in North Germany [26], has achieved a significant milestone in the field of kite power generation. They have successfully installed their first commercial system, featuring a single unit with a capacity of 150 kW, in Mauritius [27]. This installation marks a major step forward for the industry as they bring their innovative technology to the market. In addition, the company has established a small production line to further advance the production and deployment of its kite power technology [21].

Kitepower, in Figure 3.3(c), a registered trademark of Enevate BV, is a leading startup in the field of AWE [28]. Founded in 2016 by Johannes Peschel and Roland Schmehl, Kitepower builds upon the kite power research group of TU Delft, led by former astronaut Wubbo Ockels. The innovative approach of Kitepower uses up to 90% less material compared to conventional wind turbines, while achieving twice the efficiency for the same power output. Kitepower has already developed systems in a real life scenario, with an AWES with a capacity of 100 kW in Aruba [28].

Omnidea, in Figure 3.3(d), is a Portuguese company whose goal is to create an innovative airborne tethered platform using inflatable structures [29]. The platform in study is capable of generating aerodynamic lift through the Magnus effect, as it is much greater than buoyancy, making it possible to withstand wind drag while carrying heavier payloads. Additionally, by tethering the platform, power can be continuously supplied from the ground to the airborne systems, minimizing the need for frequent landings [29]. The prototype developed by Omnidea demonstrates several notable characteristics, such as the possibility of working at an altitude of 600 meters, a payload capability of 40 kg, and can sustain flight for a good period of time, as long as 24 hours [29].

3.2.7 Kite Wind Farm

AWES have demonstrated their potential suitability for smaller or remote applications, where access to traditional electricity grids may be limited [17]. However, there is also a growing interest in grouping AWES in larger-scale installations, known as kite farms. These kite farms offer exciting opportunities for harnessing wind energy efficiently and sustainably.

The performance of an AWE farm is influenced by various factors, including topography, tether length, and operational elevation angle [17]. Despite the fact AWE units have larger swept surfaces compared to conventional wind turbines, they can be positioned in closer proximity to each other due to the minimal influence of the wake effect, as the area swept is much larger than the area occupied by the kites. Consequently, this characteristic allows for increased power output within the same area; therefore, optimizing these factors becomes crucial to maximize the energy production of AWE farms.

In order to achieve continuous electricity generation to integrate the wind farm into the grid and lower the levelized cost of energy (LCOE) of the units, some advanced control strategies such as collision avoidance and coordinated collective operation must be considered [17]. These strategies help to overcome the inherent variability in power generation associated with AWES, enabling their seamless integration into the existing power grid infrastructure.

(a) Makani [24].

(b) SkySails [26].

(c) KitePower [28].

(d) Omnidea [29].

Figure 3.3: Different companies technologies

From an economic efficiency standpoint, opting to deploy a greater quantity of smaller AWE units has demonstrated clear advantages compared to solely increasing the power output of a single unit. This approach not only tackles the complexities associated with scaling up the power generation capacity of a single unit but also significantly enhances the overall robustness of the system, as, by distributing the workload across multiple units, in the event of potential failures or maintenance requirements, becomes localized, only a fraction of the overall system would be affected, safeguarding uninterrupted electricity supply while minimizing disruptions to the grid.

Therefore, it is evident the need for the optimization of AWE farm operation, taking into account the implementation of advanced control strategies, which involve complex considerations, such as minimizing distances between units and synchronising their flights within the wind farm. By addressing these aspects, it becomes possible to maximize the power generated by the farm and effectively mitigate fluctuations in electrical power output.

These optimization efforts are essential for ensuring efficient and reliable energy production, thereby enabling the widespread adoption and integration of AWE technology into the existing power grid infrastructure.

3.2.8 Working Principle of Ground-Gen Single Unit

The optimization of the layout of a set of single units and the power averaging are a complex problem to address. To maximize the power production in a given area, it is important to understand the behaviour of a single unit.

The single unit used in the UPWIND and KEFCODE Projects corresponds to a ground generation, a fixed ground station, and crosswind pattern flight operation (Figure 3.4). This working principle can be divided into two phases: the power generation phase and the retraction phase. During the power generation phase, the kite is launched into the air, and as it ascends, the winch lets out the tether [4]. The kite flies in a crosswind pattern, generating lift due to the aerodynamic forces acting on the fixed wing. The primary components of such a system include the fixed wing kite, the tether, the winch, and the generator.

As the kite moves across the wind area, the tension in the tether causes the winch to rotate. This rotational motion is harnessed by the generator, converting mechanical energy into electrical energy. The power generated by the generator can be fed into the grid or used for various applications.

Once the tether reaches its maximum length or the predetermined operating altitude, the kite transitions into the retraction phase. In this phase, the kite nosedives towards the ground station, and the winch quickly reels-in the tether. As the tether is retracted, the generator consumes a certain amount of energy to maintain tension on the tether [19]. The retraction phase is crucial for resetting the system and preparing for the next power generation cycle.

The cyclic nature of the AWES allows for continuous power generation as long as suitable wind conditions persist, having the need for take-off and landing procedures in these cases. The key advantage of using a fixed wing in AWES is its ability to maintain a stable and predictable flight pattern, resulting in consistent power generation.

By employing advanced control algorithms, it is possible to optimize the flight trajectory of the kite, making adjustments to maximize power generation efficiency and respond to changing wind conditions. These control systems play a vital role in ensuring the stability, safety, and performance of AWES with fixed wing kites [19].

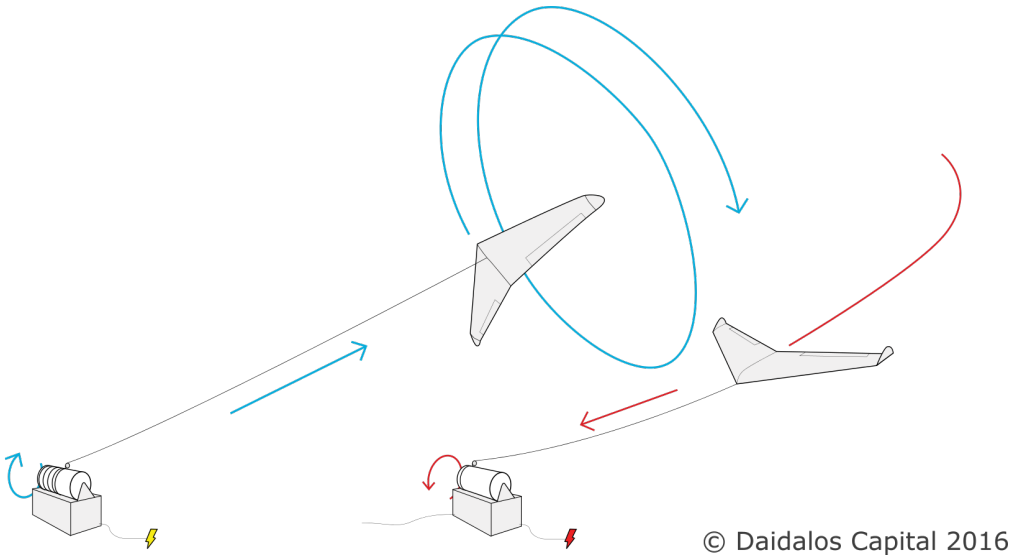

Figure 3.4: Working principle [4]

Chapter 4

Problem Formulation

In this chapter, we delve into the necessary formulation to understand the behaviour of an AWES single unit and the power produced over time. We explore the key aspects of wind and power analysis, as well as unit power output, providing insights into the factors that influence the performance of an AWES.

In the first section, we focus on wind analysis, which is essential for assessing wind resource and optimizing the operation of an AWES. We begin by examining the concept of wind shear, which describes the variation of wind speed with altitude, which helps the characterisation of wind profiles at different heights. Additionally, we discuss the wind direction, speed, and frequency analysis, providing valuable insights into the wind patterns at a specific location. Finally, to better model and interpret wind data, we introduce the Weibull Distribution, widely used to describe wind speed in a given location.

The second section of this chapter centres around the calculation of the unit power output, focusing on the mechanisms and factors that contribute to the power generation of a single unit. We start by exploring the coordinates to represent the position and orientation of the kite in relation to the wind. We further investigate the key factors influencing the power generation process, such as the roll angle and lift force. By understanding these fundamental elements, we can evaluate the instantaneous power produced by the kite, which leads to the determination of the power over time. By analysing these aspects, we can assess the overall power production of the AWES, taking into account any relevant constraints that may affect the power output and performance of the system.

Lastly, the third section also explores power measurement and evaluation to assess the performance of the kite wind farm. By analysing power data, we can gain valuable insights to support decision-making and meaningful conclusions. Besides that, power measurement allows for assessing the effectiveness and efficiency of the wind farm, enabling us to optimize its operation and maximize its power output.

4.1 Wind Analysis

Wind energy projects are heavily influenced by the unpredictable and fluctuating nature of wind, making comprehensive wind analysis a critical component of their development. Wind analysis involves the evaluation of key parameters such as wind shear, wind speed, and the Weibull distribution.

By thoroughly characterising the wind resource at a specific site, wind analysis provides valuable insights into the unique characteristics of the location and enables the optimization of available resources. It serves as a crucial factor in determining the feasibility of a project, whether involving traditional wind turbines or AWES. These studies will regard some parameters, like wind direction and wind speed, measured accurately by specialised equipment such as anemometers.

Wind analysis is fundamental to the development, implementation, and operation of wind energy projects. It furnishes essential information for informed decision-making regarding the design and functioning of wind energy technologies, enabling efficient utilisation of the available wind resource and ensuring the economic viability and sustainability of wind energy endeavours.

4.1.1 Wind Shear

Kites are deployed at high altitudes to capture strong and consistent winds. However, acquiring wind data at these elevated locations can be challenging and expensive. To address this issue, anemometers are typically used to gather wind information at lower altitudes, where they are more accessible and cost-effective.

To estimate winds at higher altitudes, we employ the wind shear model, which utilises

$$v_w(h_1) = v_w(h_0) \cdot \frac{\ln\left(\frac{h_1}{z_0}\right)}{\ln\left(\frac{h_0}{z_0}\right)}. \tag{4.1}$$

Here, $v_w(h_1)$ represents the wind speed estimate at height h_1, $v_w(h_0)$ is the wind speed at a reference height h_0, z_0 represents the terrain roughness.

While wind speeds at higher altitudes are influenced less by surface roughness, the wind shear model takes into account the impact of surface friction at lower levels. Surface characteristics and obstructions create friction, causing wind speeds to decrease nearer to the ground [30]. Consequently, the wind shear model incorporates the terrain roughness parameter, which represents the influence of surface conditions on wind velocity.

To implement the wind shear model, it is crucial to determine the value of terrain roughness [31]. If the terrain roughness is unknown, it can be calculated using the least square method, which served to estimate the parameters of a mathematical model by minimizing the sum of the squared differences between observed data points and the corresponding predicted values from the model.

The process involves fitting a mathematical model to a set of measured data points and adjusting the parameters of the model to minimize the sum of squared differences between the observed

data and the predictions of the model [31]. This iterative process allows us to find the best-fitting solution that optimally represents the relationship between variables.

In practice, we utilise real measurements of 2 different heights and calculate, regarding Equation 4.1, the wind speed at the other height. This gives the possibility to compare the estimated wind speeds to the real ones. Given this, we calculate the error between the real and estimated measurements. By calculating the error between the real and estimated measurements, we can assess the accuracy of our model. The least square method enables the minimization of the sum of squared errors, thereby ensuring a close correspondence between the estimated values of terrain roughness (z_0) and the real values.

Once we have obtained the values of terrain roughness, we can calculate the wind speeds at various heights. It is important to note that, for model simplicity, it is assumed the wind is parallel to the ground plane and remains constant over time. This concept can be visualised in Figure 4.1.

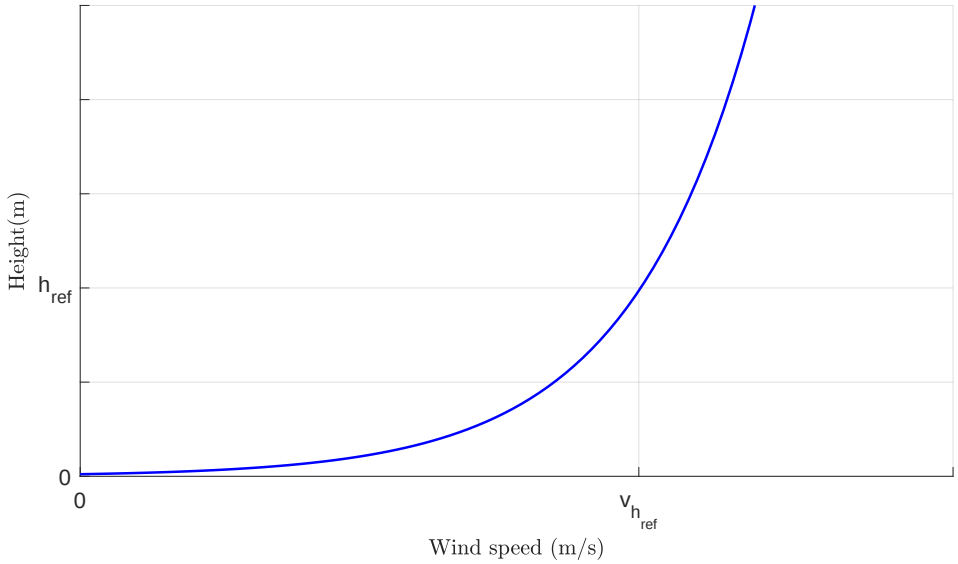

Figure 4.1: Wind shear model

The wind shear model offers a valuable technique for estimating wind speeds at higher altitudes based on measurements obtained at lower levels. By leveraging this model and accurately characterising wind shear, the design and placement of AWES, as well as the power production estimation, can be optimized, leading to a more efficient and cost-effective technology.

4.1.2 Wind Direction, Speed and Frequency

To fully understand the characteristics of a location, it is crucial to consider important parameters such as wind speed, frequency, and direction. Wind direction indicates the origin of the wind, while wind speed refers to the magnitude of the velocity. On the other hand, frequency represents

the number of times the wind blows from a particular direction or at a particular speed within a given timeframe.

The evaluation of these parameters holds significant importance in the process of assessing the wind resource, as it is essential to recognise that the wind resource varies both spatially and temporally. Therefore, it is necessary to collect data over an extended period to obtain an accurate assessment, which is generally gathered by an anemometer capturing wind characteristics over a prolonged time duration. The wind can be analysed by examining the frequency and the speed of each wind direction observed during a specific time period.

4.1.3 Weibull Distribution

Wind speeds exhibit temporal variability, including fluctuations in frequency and intensity. While wind conditions can change without prior warning, it is possible to predict the frequency distribution within a specific timeframe by analysing historical data.

To gain a better understanding of wind speed data, it is common to extrapolate a distribution that accurately represents the characteristics of the data. One such distribution widely used in wind energy applications is the Weibull distribution, named after the Swedish mathematician Wallodi Weibull [32].

The Weibull distribution is defined by three parameters: the shape parameter, the scale parameter, and the threshold. The shape parameter determines the shape of the distribution curve, while the scale parameter determines its location along the wind speed axis [33]. In the context of this study, the threshold is typically set at zero. Figure 4.2 illustrates the influence of these parameters on the aspect of the Weibull distribution.

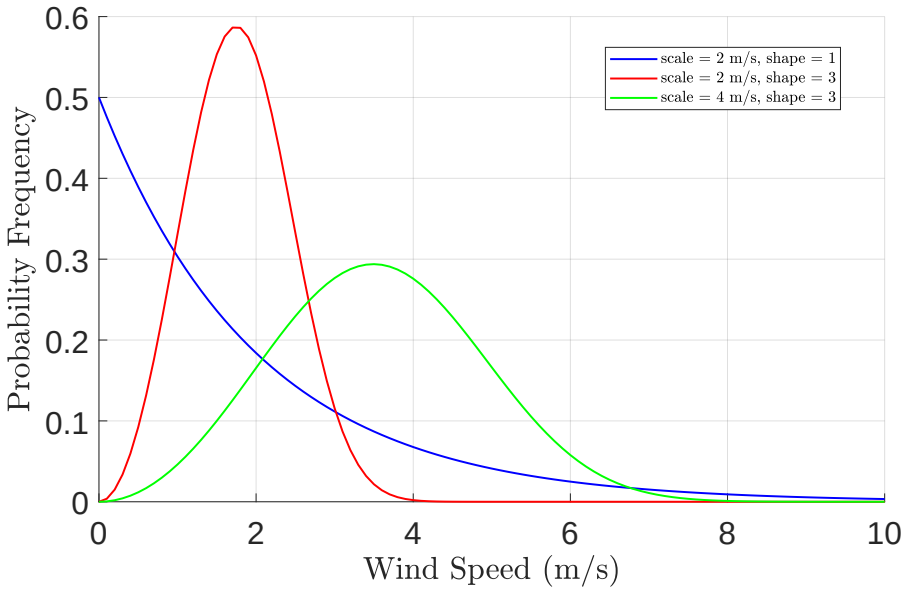

Figure 4.2: Weibull distributions

The Weibull distribution is extensively employed in wind energy applications for wind resource assessment and wind energy forecasting [33]. It serves as a powerful tool for characterising the wind resource at a specific location and is essential for designing wind energy projects. By fitting the Weibull distribution to wind speed data collected at a particular site, various aspects of the wind resource can be estimated, including the most probable wind speed and the probability of wind speeds exceeding specific thresholds, such as the cut-in and cut-out speeds relevant to unit safety and success.

4.2 Unit Power Output

To fully comprehend the operation of AWES, it is crucial to understand the underlying components and the processes involved in a single unit. In the following subsections, we will provide an overview of the essential steps and constituents that contribute to the behaviour of the kite and the estimation of the power generated over time. It is important to refer the formulation is based on [34].

4.2.1 Coordinate System

In the model, we can define the position of the kite using Cartesian coordinates (x, y, z), where the origin of the system of coordinates refers to the ground station of the unit. Here, the x-axis aligns with the wind direction, the y-axis represents the perpendicular direction of the wind, and the z-axis corresponds to the altitude.

However, a more effective approach for describing the model is to use spherical coordinates (Figure 4.3), as they offer a more intuitive representation of the position of the kite in three-dimensional space.

In spherical coordinates, the position of the kite is determined by three parameters: radial distance (r), azimuth angle (φ), and elevation angle (β).

1. Radial Distance (r): This parameter represents the straight-line distance between the ground station (origin of the coordinate system) and the kite. It measures the direct distance from the origin to the kite.

2. Azimuth Angle (φ): The azimuth angle defines the angle between the positive x-axis and the line connecting the kite to the ground station. The azimuth angle is measured in a counterclockwise direction in the xy-plane.

3. Elevation Angle (β): The elevation angle determines the vertical position of the kite relative to the ground. It measures the angle between the xy-plane and the line connecting the kite to the ground station. The elevation angle is measured from the xy-plane towards the positive z-axis.

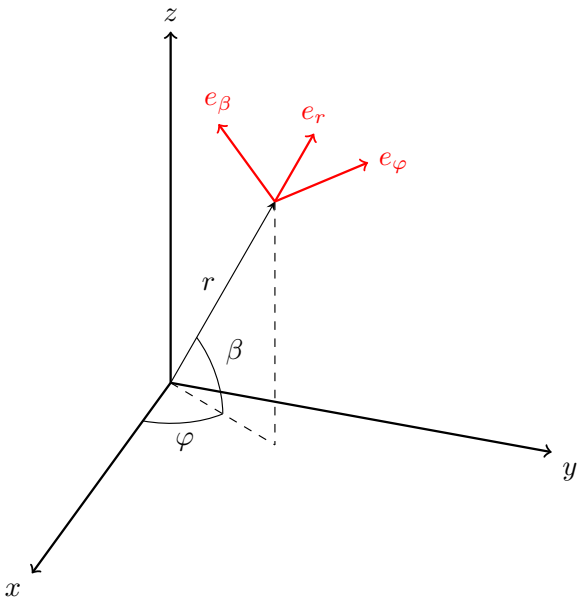

Figure 4.3: Spherical coordinates

It is possible to convert the spherical coordinates (r, ϕ, β) of a point in three-dimensional space to its Cartesian coordinates (x, y, z) using the following equations

$$\begin{aligned} x &= r\cos(\beta)\cos(\varphi), \\ y &= r\cos(\beta)\sin(\varphi), \\ z &= r\sin(\beta). \end{aligned}$$

Using these coordinates, the position of the kite can be formulated as two different components: a radial component headed outwards from the kite position and a tangential component.

4.2.2 Tangential Plane

This tangential component can be better described using a tangential plane to the kite trajectory, which is visualised in Figure 4.4.

This tangential plane τ describes the kite position in terms of φ and β, as shown in Figure 4.5. Due to the circular trajectory adopted for the study, the tangential plane allows for a simplification in order for the elevation angle β and the azimuth angle φ to be described in terms of a single angle σ. This σ defines the instant position of the kite in the circular trajectory [8]. The values of β and φ can be expressed as functions of σ using Equations 4.3. Here, $\sigma \in [0, 2\pi]$ and $\Delta\beta = \Delta\varphi$ to ensure a circular path.

$$\beta(\sigma) = \beta_0 + \Delta\beta\sin(\sigma) \tag{4.2}$$

$$\varphi(\sigma) = \Delta\varphi\cos(\sigma) \tag{4.3}$$

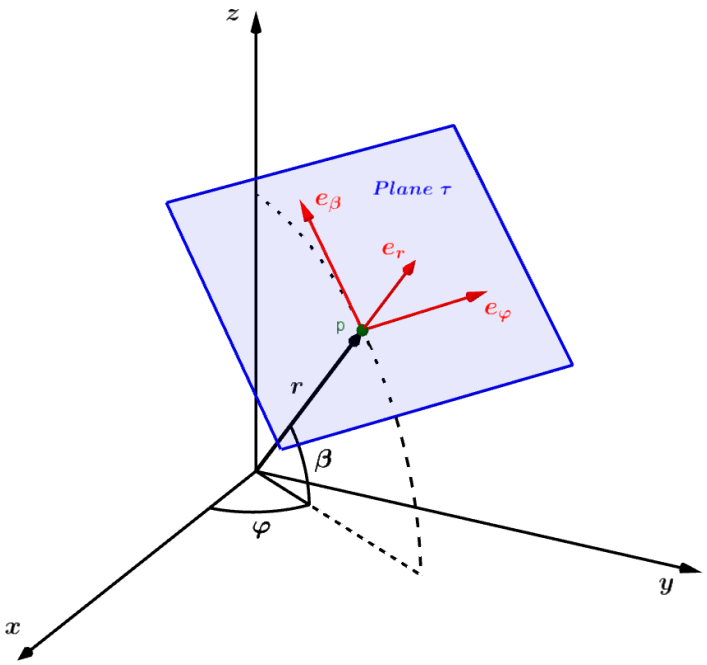

Figure 4.4: Tangential plane τ in the spherical coordinates

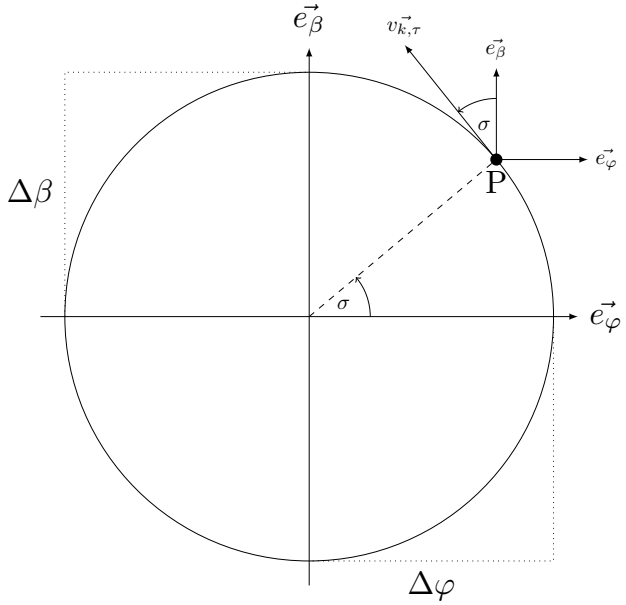

Figure 4.5: Circular trajectory in a tangential plane τ

From this, it is easier to formulate the kite velocity, which is defined by both radial and tangential components

$$\vec{v_k} = \vec{v}_{k,r} + \vec{v}_{k,\tau}\,. \tag{4.4}$$

4.2.3 Apparent Wind

In the field of AWE, the concept of apparent wind is of utmost importance. It refers to the wind experienced by the kite, i.e., apparent wind is the relative wind felt by the kite, taking into account its own motion.

Mathematically, we can express the apparent wind velocity as the difference between the wind velocity and the kite velocity [35]. This is shown in Equations 4.6 and 4.10.

The apparent wind velocity is represented by $\vec{v_a}$, which is obtained by subtracting the kite velocity $\vec{v_k}$ from the wind velocity $\vec{v_w}$ [35]

$$\vec{v}_a = \vec{v}_w - \vec{v}_k = \vec{v}_w - \vec{v}_{k,r} - \vec{v}_{k,\tau}\,, \tag{4.5}$$

which can be decomposed as:

$$\vec{v_a} = \begin{bmatrix} \cos(\beta)\cos(\phi) \\ \sin(\beta)\cos(\phi) \\ -\sin(\phi) \end{bmatrix} \cdot v_w - \begin{bmatrix} 1 \\ 0 \\ 0 \end{bmatrix} \cdot v_{k,r} - \begin{bmatrix} 0 \\ -\cos(\sigma) \\ -\sin(\sigma) \end{bmatrix} . v_{k,\tau}\,. \tag{4.6}$$

It is assumed that the tether is straight, so the kite radial velocity is equal to the tether reeling-out speed, $\dot{r} = v_{k,r}$ [35]. To better understand the relationship between the kite velocity and the wind velocity, we can define two ratios: the kite radial speed and wind speed ratio, f, and the kite tangential speed and wind speed ratio, λ.

The kite radial speed and wind speed ratio, f, is given by the equation [35]

$$f = \frac{v_{k,r}}{v_w}\,, \tag{4.7}$$

while the ratio between the kite tangential speed and wind speed, λ, can be defined as [35]

$$\lambda = \frac{v_{k,\tau}}{v_w}\,. \tag{4.8}$$

These ratios allow the decomposition of the apparent velocity of the kite relative to the wind velocity. The following equation can describe the apparent velocity

$$\vec{v_a} = \begin{bmatrix} \cos(\beta)\cos(\varphi) - f \\ \sin(\beta)\cos(\varphi) + \lambda\cos(\sigma) \\ -\sin(\varphi) + \lambda\sin(\sigma) \end{bmatrix} \cdot v_w\,. \tag{4.9}$$

Similarly to the kite velocity, the apparent wind velocity can also be divided into different components, namely a radial and a tangential one [35]

$$\vec{v_a} = \vec{v}_{a,r} + \vec{v}_{a,\tau}\,. \tag{4.10}$$

Assuming negligible gravitational and inertial forces, the ratio between the tangential and radial components of the apparent wind velocity can be expressed as the ratio of the lift and drag coefficients, denoted by c_L and c_D, respectively [35]

$$\frac{v_{a,\tau}}{v_{a,r}} = \frac{\vec{F}^{\text{lift}}}{\vec{F}^{\text{drag}}} = \frac{c_L}{c_D}. \tag{4.11}$$

From Equation 4.9, the radial component of the apparent wind velocity follows

$$v_{a,r} = (\cos(\beta)\cos(\varphi) - f) \cdot v_w. \tag{4.12}$$

Using Equations 4.11 and 4.12, we can obtain an expression for the magnitude of the apparent wind velocity [36]

$$v_a = v_w \cdot (\cos(\beta)\cos(\varphi) - f)\sqrt{1 + \left(\frac{c_L}{c_D}\right)^2}. \tag{4.13}$$

To ensure that the magnitude of the apparent wind is not negative, it is necessary to impose the following constraint

$$f < \cos(\beta)\cos(\varphi). \tag{4.14}$$

Using Equations from 4.6, we can express the tangential component of the apparent wind velocity as [35]

$$v_{a,\tau} = v_w \cdot (\cos(\beta)\cos(\varphi) - f) \cdot \frac{c_L}{c_D} \tag{4.15}$$

and

$$v_{a,\tau} = v_w \cdot \sqrt{(\sin(\beta)\cos(\varphi) + \lambda \cdot \cos(\sigma))^2 + (-\sin(\varphi) + \lambda \cdot \sin(\sigma))^2}. \tag{4.16}$$

Developing the equations, we can reach the following expression of λ

$$\lambda = a + \sqrt{a^2 + b^2 - 1 + \left(\frac{c_L}{c_D}^2\right)(b - f)^2}, \tag{4.17}$$

with a and b defined as

$$a = -\sin(\beta)\cos(\varphi)\cos(\sigma) + \sin(\varphi)\sin(\sigma),$$
$$b = \cos(\beta)\cos(\varphi).$$

To guarantee λ is positive [35], it is required to constrain the solution by

$$\cos(\beta)\cos(\varphi) < \frac{\sqrt{1+\left(\frac{c_L}{c_D}\right)^2 (b-f)^2} + f\left(\frac{c_L}{c_D}\right)^2}{1+\left(\frac{c_L}{c_D}\right)^2}. \tag{4.18}$$

4.2.4 Lift Force and Roll Angle

In order to understand the behaviour of a kite in flight, it is important to consider its intrinsic flight characteristics and the forces that act upon it such as the air density ρ, the traction force F_{tr}, and the influence of the mass of the kite m, according to [35].

The lift force $\vec{F}^{lift}$ is defined as the component of the aerodynamic force that is perpendicular to the flow direction. It contrasts with the drag force $\vec{F}^{drag}$, which is the component of the force parallel to the flow direction, as shown in Figure 4.6.

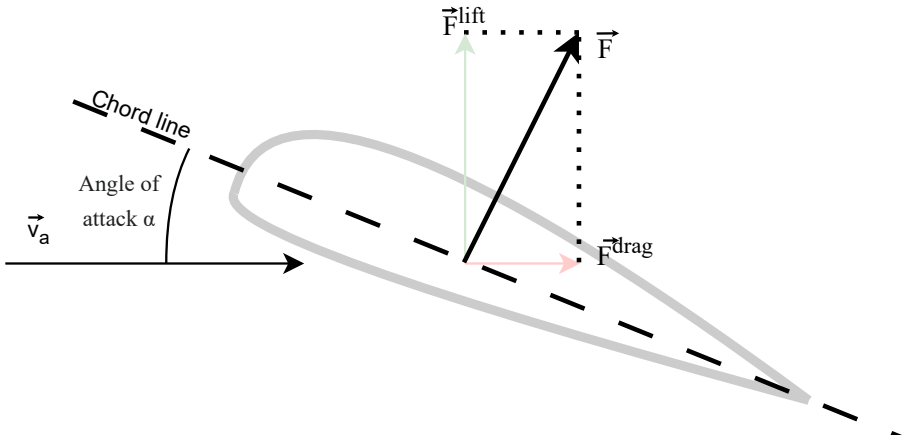

Figure 4.6: Concept of lift force

It is important to refer that the determination of the lift coefficient and the drag coefficient are dependent on the angle of attack α. For the specific purposes of this research, it is posited that the aforementioned coefficients remain invariant throughout the study.

The lift force can be expressed by the equation [35]

$$\vec{F}^{lift} = \frac{1}{2} \cdot \rho \cdot A \cdot c_L \cdot {v_a}^2. \tag{4.19}$$

Besides this, it is also very important to take into account the roll angle of the kite (ψ), as by manipulating this angle [35], we can induce a rotational motion around its longitudinal axis, resulting in a lateral force component called the Turning Lift, $\vec{F}^{lift}_{turning}$ (Figure 4.7).

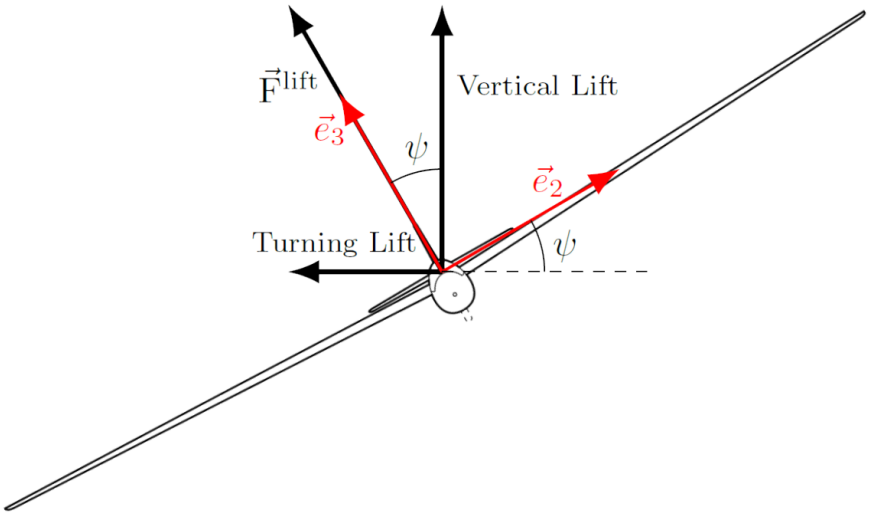

Figure 4.7: Concept of roll angle [5]

This force is essential to follow a predetermined path and must provide the necessary centripetal acceleration for the kite to trace a circular trajectory with radius $R = r \cdot \sin(\Delta\beta)$. The magnitude of the Turning Lift can be expressed as [35]

$$|\vec{F}^{lift}_{turning}| = |\vec{F}^{lift}| \sin(\psi)\,. \tag{4.20}$$

This turning lift generates a lateral acceleration that turns the kite inside the τ plane and allows it to be guided along a predetermined course [34]. This acceleration is as follows

$$a_{turning} = \frac{|\vec{F}^{lift}| \sin\psi}{m}\,. \tag{4.21}$$

Besides this, the acceleration to ensure the kite follows the predefined course is given by the centripetal acceleration $a_{centripetal}$ [34]

$$a_{centripetal} = \frac{v_k^2}{r \cdot \sin(\Delta\beta)}\,. \tag{4.22}$$

By equating Equations 4.21 and 4.22, we can derive an expression for the required roll angle [34]

$$\psi = \arcsin\left(\frac{m \cdot {v_k}^2}{|\vec{F}^{lift}| \cdot r \cdot \sin(\Delta\beta)}\right), \tag{4.23}$$

where kite velocity v_k can be computed as

$$v_k = \sqrt{v_{k,r}^2 + v_{k,\tau}^2} = \sqrt{v_w^2 f^2 + v_w^2 \lambda^2} = v_w \sqrt{f^2 + \lambda^2}\,. \tag{4.24}$$

4.2.5 Instantaneous Power

Having the previous variables sorted, it is possible to express the instantaneous power produced at every moment during the traction phase of the unit cycle [35]. The expression is given in Equation 4.25

$$P_T = \mathrm{F_T} \cdot v_{k,r} = \mathrm{F_T} \cdot f \cdot v_w = \frac{1}{2}\rho \cdot v_w^3 \cdot A \cdot c_R \left[1 + \left(\frac{c_L}{c_D}\right)^2\right] \cdot f \cdot (\cos(\beta)\cos(\varphi) - f)^2 . \tag{4.25}$$

where f, which is differentiated and equal to zero, can be computed as

$$f = \frac{1}{3}\cos(\beta)\cos(\varphi) \tag{4.26}$$

and the aerodynamic force coefficient as

$$c_R = \sqrt{c_{L,r}^2 + c_D^2} . \tag{4.27}$$

In this Equation 4.27, $c_{L,r}$ corresponds to the radial component of the lift force and may be computed as [35]

$$c_{L,r} = c_L \cos(\psi) . \tag{4.28}$$

4.2.6 Reel-out Average Power Production

Knowing the instantaneous power production at every moment, it is possible to estimate the average power production during the power production phase of the cycle. This can be achieved by integrating the instantaneous power production over the entire reel-out phase [35].

Mathematically, it can be expressed as

$$P_{tr} = \frac{\int_{r_{\min}}^{r_{\max}} \int_0^{2\pi} P_T \, d\sigma dr}{2\pi (r_{\max} - r_{\min})} . \tag{4.29}$$

Breaking down the equation

$$P_{tr} = \frac{\int_{r_{\min}}^{r_{\max}} \int_0^{2\pi} \frac{1}{2} \cdot \rho \cdot A \cdot v_w^3 \sqrt{(c_L \cos(\psi))^2 + c_D^2} \left(1 + \left(\frac{c_L}{c_D}\right)^2\right) \cdot f \cdot (\cos(\beta(\sigma))\cos(\varphi(\sigma)) - f)^2 \, \mathrm{d}\sigma \mathrm{dr}}{2\pi (r_{\max} - r_{\min})} . \tag{4.30}$$

4.2.7 Reel-in Average Power Consumption

In addition, it is also possible to estimate the necessary power that is consumed in order to retract the tether and restart the cycle.

This power consumption during the reel-in phase can be calculated using the following equation [35]

$$P_{re} = \frac{1}{2}\rho \cdot A \cdot v_w^2 \cdot c_D \cdot v_{re} \left(\left(\frac{v_{re}}{v_w} \right)^2 + 2\frac{v_{re}}{v_w} \cos(\beta_{re}) + 1 \right). \tag{4.31}$$

4.2.8 Average Power Production

Reaching this point, it is possible to estimate the power production of the kite along the entire cycle.

The process of converting power is not fully efficient, and therefore those losses in this problem must also be considered. During the traction phase, the efficiency of converting mechanical to electrical power is denoted by η_{tr}, and during the retraction phase, the efficiency of converting electrical to mechanical energy is represented by η_{re} [35].

The discrete sets of v_w, which represent potential wind speed values, and β, which represents the kite's elevation angle, are used to model the potential wind speed values of the kite.

For each combination of β (elevation angle) and v_w (wind speed) values, the optimal traction and retraction speeds, v_{tr} and v_{re}, are determined to maximize power production throughout the cycle (P_c). This allows us to calculate P_c, which represents the average power output over an entire cycle. According to [35], P_c of a single unit can be obtained using the following equation

$$P_c = \frac{E_{tr} - E_{re}}{t_{tr} + t_{re} + t_{tran}} = \frac{\frac{\eta_{tr} P_{tr} \cdot (r_{\max} - r_{\min})}{v_{tr}} - \frac{\eta_{re} P_{re} (r_{\max} - r_{\min})}{v_{re}}}{\frac{r_{\max} - r_{\min}}{v_{tr}} + \frac{r_{\max} - r_{\min}}{v_{re}} + t_{tran}}. \tag{4.32}$$

4.2.9 Constraints

There are some constraints to take into account in this process in order to have a feasible solution to the problem. These restrictions include altitude, roll angle, and elevation constraints.

4.2.9.1 Altitude

It is important to consider the height constraint, which sets a limit on the maximum altitude that the kite can reach during its flights [36]. This constraint, which may be related to safety regulations in aviation, is as follows

$$L_{\max} \sin(\beta) \leq z_{\max}. \tag{4.33}$$

4.2.9.2 Roll Angle

One of the most crucial elements that affect the overall performance of the kite wind farm is the roll angle (ψ). This occurs because a single unit runs an entire lap significantly slower having a low roll angle, implying that it occupies a larger space. On the other side, a high roll angle will significantly narrow the lap, affecting how many units are needed.

In order to make the solutions of the implementation realistic, it is mandatory to limit the roll angle to a maximum, so it will forbid extremely narrow circular trajectories, which leads to an increased number of kites. Therefore, this limitation provides feasible solutions, with realistic values of roll angle.

Besides this, the roll angle introduces a tangential component to the lift force (turning lift), as explained previously, which also reduces the radial component, which is the component responsible for energy production. Therefore, it is not recommended to use excessively high roll angles

$$\psi \leq \psi_{\max} . \tag{4.34}$$

4.2.9.3 Elevation Angle

The elevation angles (β) are a further restriction that must be taken into consideration. This concern is to ensure the kite's continuation in the air so that it can be contained within the working area.

For the kite to remain airborne and not touch the ground, it is necessary to implement a minimum value of elevation. Besides that, the upper limit ensures that the kite stays within a workable range and prevents it from gaining an excessive amount of elevation [36]

$$\beta_{\min} \leq \beta \leq \beta_{\max} . \tag{4.35}$$

4.3 Evaluation Metrics

Accurate power analysis is crucial for evaluating the performance of an AWES and making informed decisions. In this section, we dig into the various aspects of power measurement and metrics that are essential for understanding the behaviour of an AWES and optimizing its operation.

These metrics provide comprehensive insights into the performance, efficiency, and viability of AWES, supporting informed decision-making processes in their development and deployment.

4.3.1 Power Curve

One of the fundamental components of power analysis is the power curve, which provides valuable insights into the relationship between wind speed and the corresponding power output of the system. The power curve graphically represents the performance of the system and can be visualised as a plot of power output against wind speed.

At very low wind speeds, the power output of the AWE unit is nearby zero, indicating that the system is unable to generate significant power. As the wind speed increases, the power output of the unit also increases, reaching a maximum at the nominal power level when in traction phase.

This maximum power represents the nominal capacity of the system, beyond which it cannot deliver any additional power.

However, regarding higher values of wind speed, the overall power output starts decreasing. This is due to the fact that the power production continues in the value of nominal power, while the power consumption of the retraction phase continues to increase. The power curve can be seen in Figure 4.8.

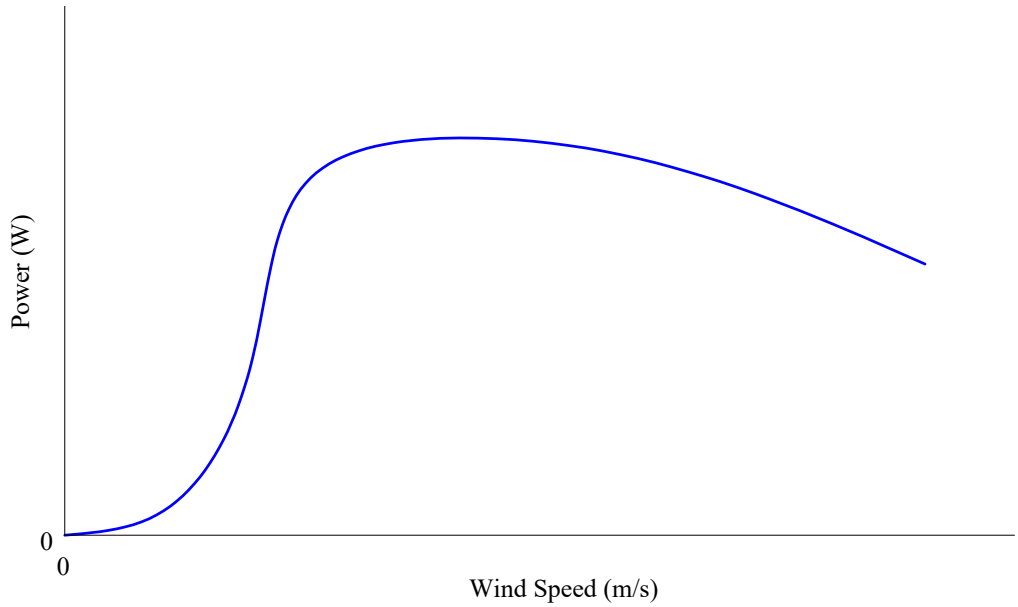

Figure 4.8: Illustration of typical power curve of an AWES

4.3.2 Cut-in and Cut-out Speeds

In addition to understanding the power curve, it is crucial to address certain factors that can affect the output of an AWES. One important aspect is the concept of cut-in and cut-out speeds.

The cut-in speed refers to the minimum wind speed at which the AWE units begin to generate power [37]. Below this speed, the units remain inactive to ensure their safety and prevent damage during situations of insufficient wind.

Conversely, the cut-out speed represents the maximum wind speed at which the units shut down and interrupt their operation [37]. This safety measure has the goal of protecting the unit from extreme weather conditions, which could pose risks to the integrity of the AWE unit.

By establishing appropriate cut-in and cut-out speeds, the AWES can operate within a safe and efficient range of wind conditions, maximizing power generation while ensuring the longevity of the system.

4.3.3 Average Power Output and Annual Energy Production

To analyse the overall performance of a kite wind farm, a crucial measure is the Average Power Output (P_{avg}). This can be obtained by averaging the power output over a given period, such as a year. The average power output provides an indication of the typical power generation capability of the system and is an important metric for assessing its efficiency.

Furthermore, the annual energy production (AEP) of a kite wind farm is a key parameter that quantifies the amount of electrical energy generated by the AWES over the course of a year [38]. The AEP is typically expressed in watt-hours (Wh) and can be calculated by multiplying the average power output (P_{avg}) of a single unit by the total number of hours in a year (8760). The equation to determine the AEP is as follows

$$\mathrm{AEP} = P_{avg} \times 8760 \quad (\mathrm{W\,h})\,. \tag{4.36}$$

The AEP provides a valuable estimate of the energy production potential of the wind farm and is an essential parameter for evaluating its economic viability and contribution to the overall energy system.

4.3.4 Capacity Factor

The Capacity Factor (CF) is another important metric used to assess the performance and efficiency of a kite wind farm. It measures the actual electrical power produced by the kite wind farm relative to the maximum power it could potentially produce at peak capacity. The CF is calculated by dividing the P_{avg} by the nominal power P_{nom} of the AWES

$$\mathrm{CF} = \frac{P_{avg}}{P_{nom}}\,. \tag{4.37}$$

4.3.5 Equivalent Hours

Equivalent hours ($\mathrm{Hours_{eq}}$) is a measure that helps understand the average power production of a wind farm and its relationship with its maximum power. It represents the number of hours at maximum power that would be required to generate the same amount of energy as the average power output over the course of a year.

The calculation of equivalent hours involves dividing the average power output P_{avg} by the maximum power P_{max} and multiplying the result by the total number of hours in a year

$$\mathrm{Hours_{eq}} = \frac{P_{avg}}{P_{\mathrm{max}}} \times 8760 \quad (\mathrm{h})\,. \tag{4.38}$$

4.3.6 Power Density

Power Density (PD) is a metric that allows for the assessment of the energy production potential of a wind farm relative to the available land area. It provides insights into the energy efficiency and utilisation of the wind farm per unit area.

To calculate PD, the annual energy production (AEP) is divided by the terrain area. The equation for power density is as follows

$$\mathrm{PD} = \frac{\mathrm{AEP}}{A_{Land}} \quad (\mathrm{Wh\,m^{-2}}). \tag{4.39}$$

The power density metric helps determine how effectively the wind farm utilises the available land area to maximize energy output. A higher power density indicates a more efficient use of the land, resulting in a greater energy output per unit area.

4.3.7 Deviation of Power

Finally, Deviation of Power (ΔP) is a significant measurement that provides insights into the stability and magnitude of power output fluctuations in a wind farm. It indicates the variability of power generation and can be useful for assessing the reliability and performance of the AWES wind farm.

The deviation of power is calculated as the difference between the maximum power ($P_{\max}$) and the minimum power ($P_{\min}$) generated by the wind farm

$$\Delta\mathrm{P} = P_{\max} - P_{\min} \quad (\mathrm{kW}). \tag{4.40}$$

A lower deviation of power suggests a more stable and consistent power generation, while a higher deviation indicates larger fluctuations and potential issues.

Chapter 5

Kite Wind Farm Design

Understanding the operational principles of a single unit provides a foundation for comprehending the purpose and significance of a kite wind farm as, in a real-world setting, they are essential to the implementation of AWES.

The goal of an AWES farm is to generate electricity and efficiently deliver it to the grid. However, the complexity of wind farm optimization in AWES poses significant challenges that must be addressed in order to ensure safe and reliable operation, as well as the most efficient operation possible [17].

AWES farm optimization is inherently challenging due to a number of reasons. To begin with, the constant change of wind patterns generates uncertainties that demand real-time adaptation and management of the units. Wind speeds and directions may alter significantly at various altitudes, leading to the implementation of algorithms and control systems to optimize the flight trajectories and alignments of the units for a greater energy harvest. Furthermore, the irregular character of the units contributes to the complexity of the problem. Unlike traditional wind farms that rely on fixed wind turbines, AWES farms utilise a group of units to capture wind energy at higher altitudes, which results in greater degrees of freedom of the behaviour of the unit and, as a result, higher levels of complexity in the overall wind farm control to ensure everything works properly.

In this study, our primary focus is on kite wind farms based on Ground-Gen systems. However, it is essential to acknowledge that the insights gained from this research can be extended and applied to Fly-Gen systems as well, due to the eventual take-off or landing procedures this type of system might as well have to do.

Furthermore, the coordination of multiple units presents challenges in terms of communication and synchronisation. Efficient collaboration among the units is critical to ensure optimal energy production while maintaining safe operating conditions. To overcome these problems, it may be necessary to include some strategies, including the alteration of the alignments of the units, flying characteristics, and power outputs of each single unit in order to optimize energy generation and minimize potential conflicts.

The power generation capacity of a kite wind farm is closely related to the power output of every single unit within the farm. There is a trade-off between maximizing power production per

unit and the number of units that can be accommodated within a given area. While increasing the power output per unit may result in higher overall power generation, it also requires more space, limiting the number of units that can be installed within a given terrain. This trade-off poses one of the biggest challenges in wind farm design and optimization. Therefore, finding the right balance between power output per unit and the number of units that can be installed is crucial to maximizing the overall power generation of the wind farm.

The levels of permitted overlap within a kite wind farm also have an influence on the number of units that can be accommodated. When establishing the spacing between units, there are multiple approaches to consider. A possibility is to have independent areas for each unit that do not overlap. Since there is no sharing of space between units, the layout design is simplified. Alternatively, if the unit areas contact, collision avoidance strategies are required to ensure the proper operation of the wind farm, with the added benefit of allowing for a more compact arrangement of units to maximize power output efficiency. The most complex approach involves the sharing of space between units using conic envelopes. This allows for more efficient use of space but introduces additional challenges regarding unit positioning and optimization to avoid overlapping and maintain optimal power generation.

The different levels of overlap between units within a kite wind farm also have an influence on the number of units that can be accommodated. When determining the spacing between units, several approaches can be considered, each with its own advantages and drawbacks. In the case of no overlap, there is no risk of kite collisions. However, this approach requires each unit to occupy a larger area of the terrain, potentially limiting the number of units that can be installed within the wind farm. Alternatively, if the kites circulate in the same space, units can be placed closer to each other. However, this approach increases the risk of kite collisions, requiring additional control to ensure safety and prevent accidents. An intermediate approach to consider involves sharing the ground areas between units, while ensuring that the kites do not circulate within the same space.

The safety of the units as well as the overall integrity of the AWES farms are vital factors to consider. One of the most important safety concerns is avoiding collisions between units and their tethers or kites. To avoid this danger, it is critical to maintain minimum distances between units while taking their flight paths and operational characteristics into account. By optimizing the layout and spacing of the units, the potential for collisions can be minimized, ensuring the safe operation of the wind farm. Nevertheless, by employing a distance minimization method, it is possible to optimize the distance between units, maximizing the use of available terrain while still meeting safety requirements.

Another key part of kite wind farm optimization is assuring the quality of the electrical output of the AWES units. The cyclical nature of energy production and consumption in individual units might cause electrical output irregularities. When these anomalies are scaled up to the wind farm level, they might have a negative impact on the stability and reliability of the grid connection. To address these issues, numerous strategies can be used to reduce deviations and maintain a smooth and consistent electrical output. One approach is to synchronise the flight cycles of the units, ensuring coordinated energy production and consumption patterns. By optimizing flight

synchronisation, the kite wind farm can achieve a more predictable and balanced electrical output, hence improving the stability of the grid connection and eventually reduce costs in the structural infrastructures.

5.1 Trade-off Between Number of Units and Unit Power

To understand the trade-off between units and unit power within a kite wind farm, it is crucial to consider the spatial requirements and operational characteristics of each individual unit.

The area of operation for each unit is defined by a conical-shaped range, which is influenced by factors such as the length of the tether (r), the elevation angle of the tether (β), and the azimuth angle deviation ($\Delta\varphi$) [36] and adjusting these parameters can have a significant impact on the efficiency and power production of a single unit. In the following Figure 5.1 it is possible to visualise the envelope the unit occupies.

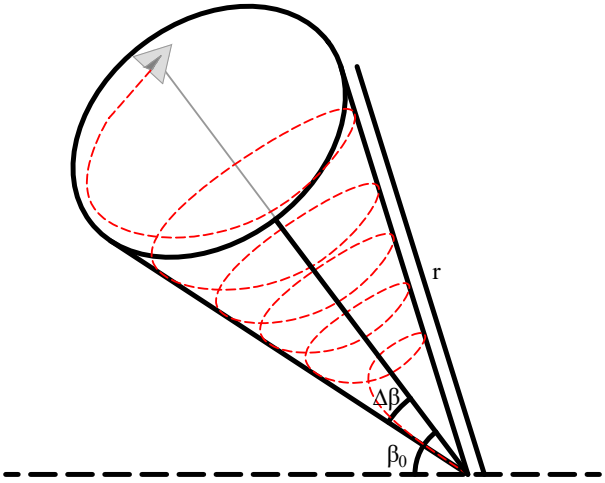

Figure 5.1: Flight envelope

On one hand, a smaller β combined with a larger $\Delta\varphi$ can lead to increased power production by maximizing the exposure of the single unit to the best characteristics for better production, as this configuration allows the unit to capture a larger cross-sectional area of wind.

However, in the context of a kite farm, the primary objective is to maximize the overall power output by optimizing the utilisation of the available area. This means that solely focusing on maximizing the power of individual units may not be the most effective approach.

By adjusting β and $\Delta\varphi$, it is possible to reduce the volume occupied by each unit. This reduction in the volume of each unit enables a higher density of units within the wind farm, ultimately leading to an increased total power output. However, it is essential to find the right balance between the number of units and their power-generating capabilities to optimize the overall performance of the kite wind farm.

5.2 Level of Permitted Overlap

The level of permitted overlap is another crucial factor in the design and implementation of a kite wind farm, as it significantly impacts the number of units that can be accommodated within a given terrain. To tackle this challenge, three main approaches can be employed to define the spacing between units, taking into consideration the area swept by the kite in the air and viewed from the top.

The first approach involves allocating distinct regions for each unit, as the areas of the envelopes projected to the ground are disjointed from each other. In this approach, the wind farm is divided into separate areas, with each area assigned to an individual unit, which simplifies the layout design process, as there is no need to account for unit interactions or collision avoidance. Here, each unit operates independently within its designated area, allowing for straightforward installation, maintenance, and control. However, this approach may result in a less dense arrangement of units, limiting the number of units that can be installed within the given terrain. This type of approach can be visualised in Figure 5.2, where each unit is represented by a designated region on the ground [39].

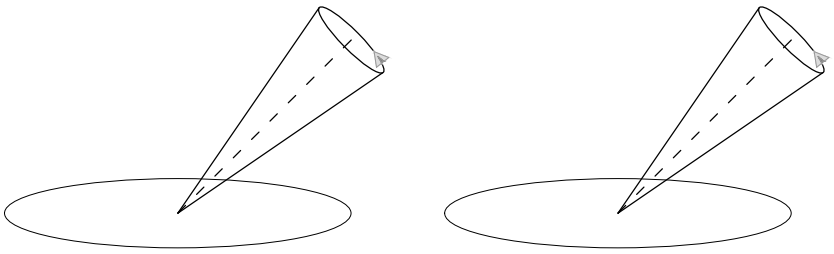

Figure 5.2: Approach with independent regions

The second approach allows for ground areas of the units to overlap while ensuring that the flight envelopes representing the swept volume of the kites for a given direction do not intersect with the flight envelope of the following unit. While the ground areas assigned to each unit can partially overlap, which provides flexibility in unit placement, it also introduces a higher level of complexity compared to non-overlapping ground areas as they require implementing collision avoidance strategies, particularly when wind direction changes occur. For that reason, the movement of units must be carefully coordinated to avoid collisions and ensure safe and efficient operations. By carefully coordinating the movement of units and avoiding collisions, this approach enables a more compact arrangement of units, potentially increasing the overall power generation capacity of the wind farm. Figure 5.3 depicts an example of this approach, illustrating the overlapping regions of the workspace cones of the units [39].

The third approach represents the most complex and terrain-optimized layout design. In this approach, both the ground areas assigned to each unit and the flight envelope intersect with the envelope of the following unit. Thus, this approach maximizes the utilisation of available terrain

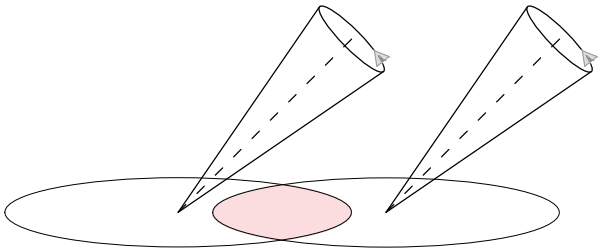

Figure 5.3: Approach with intersecting ground areas

and allows for the closest possible placement of units. However, implementing this approach requires advanced control over kite flight and precise coordination among the units to ensure the kites remain airborne, as well as safe operations within the kite farm. Figure 5.4 provides a visual representation of this strategy, showcasing the intersecting regions of the workspace cones of the units [39].

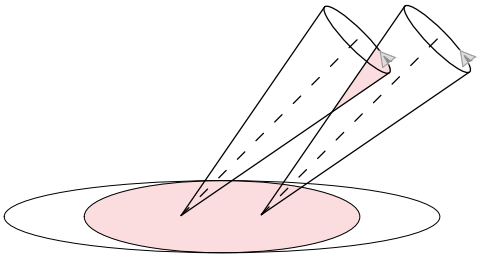

Figure 5.4: Approach with intersecting workspace regions

It is important to note that the approach used in this study is the second one, which involves overlapping ground areas, but not flight envelopes.

5.3 Distance Minimization

Distance minimization is an essential component of the safety precautions applied in the operation of an AWES farm. While it may be attractive to keep huge distances between units to reduce potential threats, this method might result in severe land waste (Figure 5.5(a)). Therefore, a method of distance minimization is employed with the primary objective of bringing the units closer together, thereby maximizing land utilisation and ultimately enhancing the power output of the wind farm.

In the context of conventional wind turbine farms, keeping a significant distance between units is frequently emphasized to reduce wake effects. However, wind farms using AWES present an alternative point of view. Given the relatively small area occupied by each individual unit compared to the airspace swept by the kites, the wake effect in AWES are negligible, and therefore, opens up the opportunity to reduce the separation distances without compromising efficiency. However,

it is crucial to consider the minimum distances required in AWES farms to address collision risks among units, including the kites and tethers. These distances are necessary due to the inherent freedom of movement exhibited by these units. By adopting an optimized distance minimization approach, it becomes possible to effectively exploit the available terrain and accommodate a greater number of units within the wind farm.

By strategically positioning the units at optimized distances, the wind farm can achieve a higher power output potential. This is due to the increased number of units that can be accommodated within a given land area, resulting in enhanced energy capture from wind resources.

It is crucial to remember that while minimizing distance may increase power output, it is important to maintain a balance between closeness between units and safety. For this reason, it is important to have a thorough understanding of the operational characteristics, flight dynamics, and potential dangers of tether or kite entanglements before determining what distances are appropriate for separation. The result assures that the wind farm operates within a safe operating envelope while optimizing the advantages of distance reduction.

From a top perspective, it becomes possible to delineate specific areas, with the ground station of the unit as the centre where the kites can circulate. To determine the appropriate spacing between units, two distinct approaches can be employed.

The first approach entails establishing a circular range around each unit, ensuring an equal distance on all sides (Figure 5.5(b)). This straightforward strategy serves as a basis to define the required spacing between units within the wind farm. Using this circular range strategy, it is possible to efficiently organize the general structure of the wind farm by keeping a constant spacing between neighbouring units.

Alternatively, the second approach takes into account the unique wind characteristics of the specific area. In this case, an elliptical-shaped area is designated for the units (Figure 5.5(c)). The dimensions of the ellipse are determined by analysing the prevailing wind patterns inherent to the location, which provide insights into the frequency and distribution of wind directions. Consequently, the major axis of the ellipse aligns with the most frequent wind directions, while the minor axis corresponds to the least frequent ones. This results in variations in power generation due to the varying tether lengths in different regions of the ellipse. The unit produces less energy when operating in the minor axis region due to the shorter tether length, but it compensates by generating a greater amount of power in the major axis region. Overall, this optimization strategy ensures that the energy generation of the unit is maximized, as the region near the major axis experiences significantly more frequent wind conditions compared to the region near the minor axis. The choice of employing an ellipse instead of a simple circle is justified by the increased energy production potential, as the kite range of each unit is tailored to the specific characteristics of the local wind patterns, while enabling a greater number of units within the same dimensions of the terrain.

It is important to refer that, for this study, it is considered the second approach. The distance between units can be guaranteed by assuring certain distances as d_1, d_2, d_3 shown in Figure 5.6.

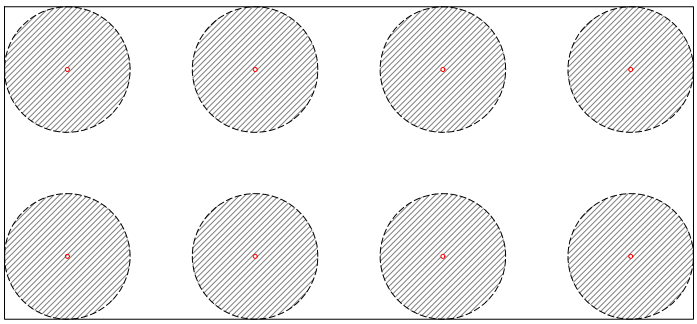

(a) Distances between units in a terrain (8 units)

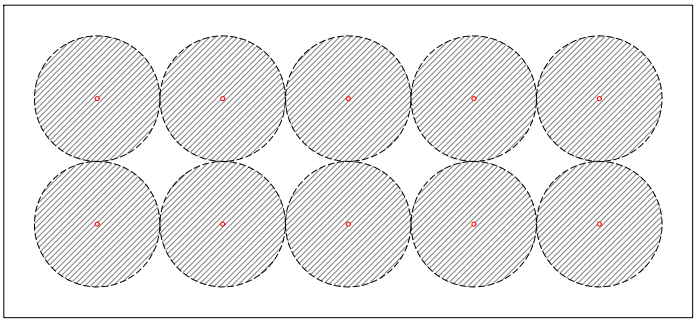

(b) Minimization of distances between units in a terrain (10 units)

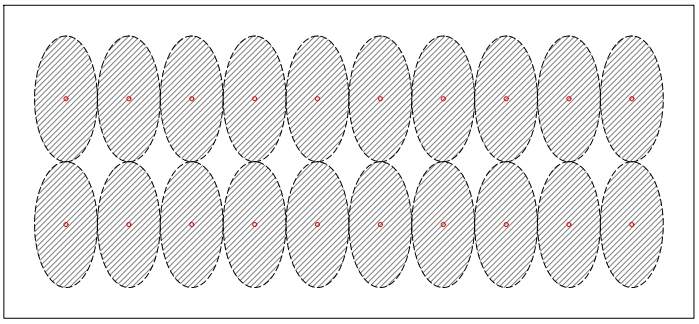

(c) Use of ellipses according to wind characteristics of the terrain (20 units)

Figure 5.5: Different patterns for distance minimization [6].

These distances between units can differ according to the wind direction to guarantee a better efficiency of the terrain used [36].

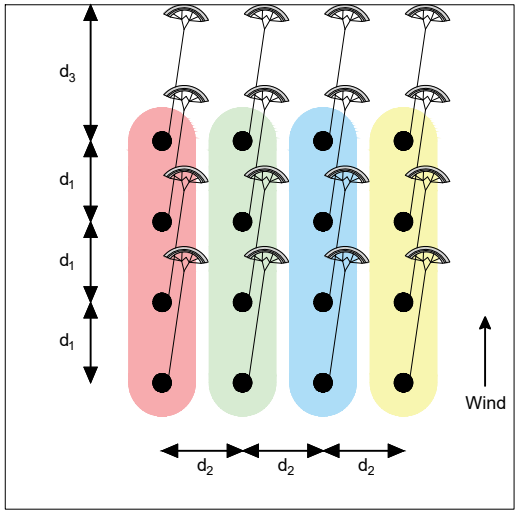

Figure 5.6: Distance minimization between units calculations

The distance d_1 is related to the distance between 2 units aligned with the wind direction 5.1

$$d_1 = \frac{L_{\max}}{\sin(\beta - \Delta\beta)\left[\frac{1}{\tan(\beta-\Delta\beta)} + \frac{1}{\tan(\beta+\Delta\beta)}\right]}. \tag{5.1}$$

To consider the distance between the last unit and the border in the wind direction, this can be calculated using the distance d_3 described by 5.2

$$d_3 = L_{\max}\cos(\beta - \Delta\beta). \tag{5.2}$$

In a perpendicular direction to the wind, the distances are described by the following Equation 5.3

$$d_2 = 2L_{\max}\sin(\varphi). \tag{5.3}$$

After these considerations, it is important to refer that in this study the spacing between units is determined by calculating the maximum distance between d_1 and d_2, as shown in the following equation

$$d = \max(d_1, d_2). \tag{5.4}$$

Once the spacing between units has been determined, it is crucial to carefully consider the layout pattern to be employed within the wind farm, as this decision plays a significant role not only in the appearance of the farm but also in the overall performance and efficiency of the system.

A commonly used pattern is the square layout, where the units are aligned in a square format (Figure 5.7(a)). However, it is important to note that employing a square pattern does not guarantee

every unit is distanced by the minimum distance possible, as the diagonal distance between two opposite vertices of the square is $\sqrt{2}d$, where d represents the desired minimum distance [6]. It is possible to estimate the number of units regarding the land dimensions and the defined distance between units. In a square layout, the number of units is given by the following equation

$$n_{\text{sq}} = \left[\frac{L_{\text{land}} - 2d_3}{d} + 1\right] \cdot \left[\frac{W_{\text{land}} - 2d_3}{d} + 1\right]. \tag{5.5}$$

In contrast, an alternative approach is to configure the wind farm layout in the form of a hexagon, or a group of equilateral triangles. By using a hexagonal pattern composed of overlapping equilateral triangles (Figure 5.7(b)), each unit is spaced precisely at the calculated minimum distance d [6]. This layout pattern ensures that all units are arranged in an evenly distributed manner, and it is the densest packing pattern possible. For a hexagonal layout, the number of units is given by

$$\begin{aligned} n_{\text{hex}} = &\left[\frac{L_{Land} - 2d_3}{\sqrt{3}d} + 1\right] \cdot \left[\frac{W_{Land} - 2d_3}{d} + 1\right] \\ &+ \left[\frac{L_{Land} - 2d_3 - \frac{\sqrt{3}}{2}d}{\sqrt{3}d} + 1\right] \cdot \left[\frac{W_{Land} - 2d_3 - \frac{d}{2}}{d} + 1\right]. \end{aligned} \tag{5.6}$$

It is important to note that even though the square and hexagonal layouts are described as the potential options, the suitability of different layout patterns, such as hybrid configurations, may vary depending on the specific characteristics of the wind farm area, because factors such as the shape and irregularity of the terrain in study can significantly influence the choice of the layout pattern.

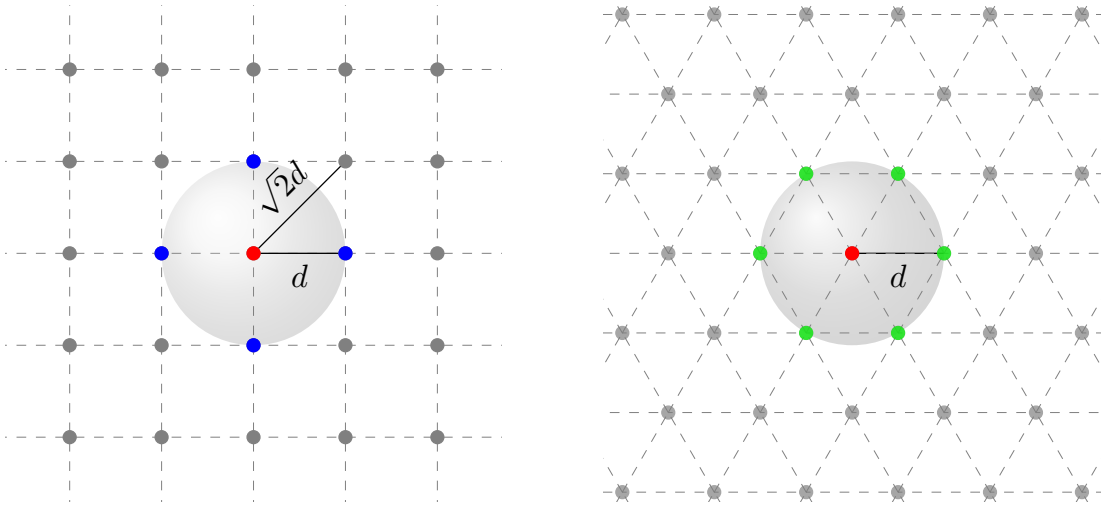

(a) Square pattern. (b) Hexagonal pattern.

Figure 5.7: Different patterns for distance minimization [6].

5.4 Power Averaging and Smoothing

The successful implementation of wind farms heavily relies on the reliable and consistent connection between the wind farm and the electrical grid [40].

5.4.1 Problem Explanation

In the case of AWES, each unit operates in a cyclic manner, with distinct phases of energy generation and consumption as the kite moves relative to the ground station [7].

During the reel-out phase, the kite flies in a crosswind pattern, generating energy as it moves away from the ground station. As the kite reaches the maximum length of the tether, a transition phase occurs where the kite reaches the desired retraction elevation angle and reorients itself, pointing its nose towards the ground station in preparation for the reel-in phase. In this transition phase, the power output is zero, as no energy is being produced or consumed. Afterwards, in the reel-in phase, the kite approaches the ground station, consuming energy to maintain tension in the tether. This completes one cycle, which can be seen in Figure 5.8, and the process starts all over again. It is important to note that for the purposes of the model, the power values are equal to the average power output in each phase.

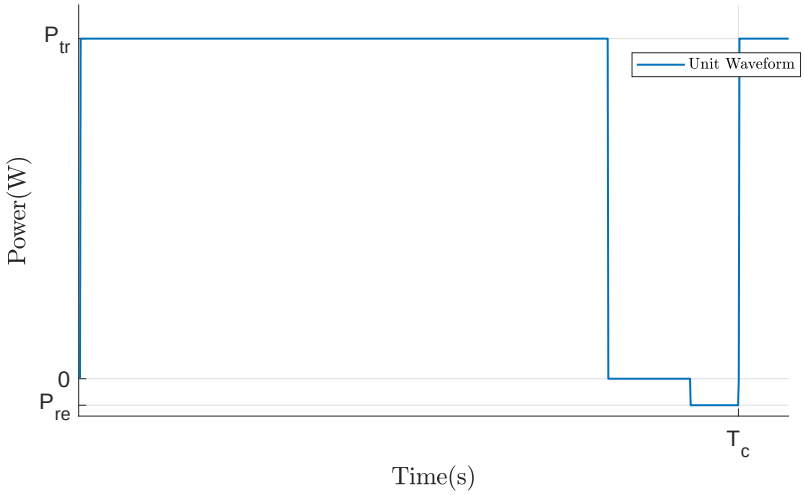

Figure 5.8: Single unit power waveform

These cyclical fluctuations in power production cause variations in the overall performance of the AWES system over time. Besides this, the power output varies between negative and positive values over time, which implies a need for storing the energy in the production phase or the need to import that energy from the grid. This phenomenon worsens the efficiency of the system. Although variances regarding a single unit may be minor, when compounded throughout a wind farm with several units, these changes can become significant and cause issues in maintaining a reliable connection to the grid, as visualised in Figure 5.9. The resulting changes in power production have

the potential to influence grid stability and dependability, resulting in unfavourable disruptions. To address these challenges, it becomes imperative to identify and implement suitable solutions that can mitigate the deviations in power output and ensure a steady bulk output of the farm.

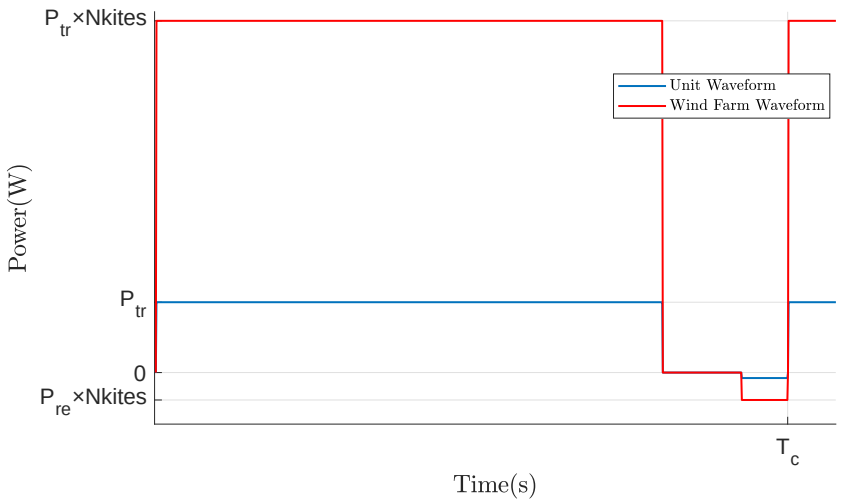

Figure 5.9: Wind farm power waveform without averaging strategies

5.4.2 Solutions

To tackle the aforementioned challenges, various approaches can be explored. In this subsection, we talk about the different approaches for this problem, namely a coordinated collective operation and an independent operation for each unit.

5.4.2.1 Synchronised Operation with Grouped Phase Shifts

One promising solution involves defining a conic-shaped region where the kite operates during the traction phase, as discussed in previous chapters. Within this defined region, the kite efficiently generates energy while moving away from the ground station. However, a critical issue arises during the retraction phase when the kite operates at a very high elevation angle, placing it outside the designated single unit area.

This situation introduces a possibility of collision when neighbouring units are in the traction phase while others are in the retraction phase. This collision risk arises because the retraction phase occurs within the power zone of adjacent single units. In essence, the retraction phase of one unit overlaps with the power zone of another unit, increasing the likelihood of kite collisions. A visual representation of this scenario can be observed in Figure 5.10.

To mitigate this risk, it is necessary to synchronise the units when they align with the wind direction. By synchronising the operational phases of the units, potential collisions can be avoided.

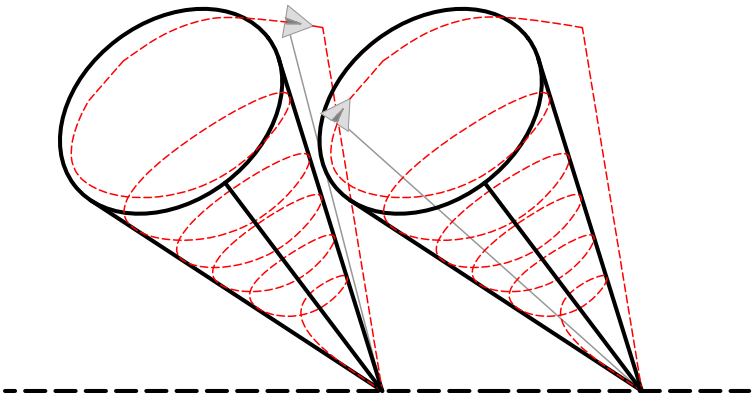

Figure 5.10: Illustration of utilising the retraction elevation angle out of the conic-shaped region.

This synchronisation ensures that neighbouring units do not enter conflicting phases simultaneously, reducing the chances of kites crossing paths.

According to [40], for wind farms with a squared layout (*nxn*), the alignment of wind farms gives rise to two extreme possibilities based on the wind direction. The first scenario occurs when the wind direction is orthogonal to one of the sides of the wind farm, while the second scenario arises when the wind aligns with the diagonal of the squared layout.

In the case of orthogonal wind alignment, synchronisation is determined by aligning the units into columns. Each column consists of n synchronised units, where n represents the number of units in each column. The synchronised units within each column work concurrently, contributing to the efficient operation of the wind farm. In the case of orthogonal wind alignment, the phase shifts between groups can be calculated by

$$\Theta = \frac{T_c}{n}. \tag{5.7}$$

For diagonal wind alignment, the phase shifts can be derived by doubling the cycle duration and dividing it by the number of columns

$$\Theta = \frac{2T_c}{n}. \tag{5.8}$$

In [40], diagonal winds result in periodic large oscillations in power output. This behaviour can be attributed to the synchronisation pattern where columns with varying numbers of units operate simultaneously, as the groups can differ from n to 1 single units.

In the case of diagonal wind alignment, an alternative synchronisation pattern is proposed by [7]. Unlike the varying numbers of units in different columns observed in the previous approach, this modification suggests matching the inner columns with the outer columns. This synchronisation pattern ensures the same number of groups as in the orthogonal wind direction, maintaining a constant number of single units in each group, as seen in Figure 5.11.

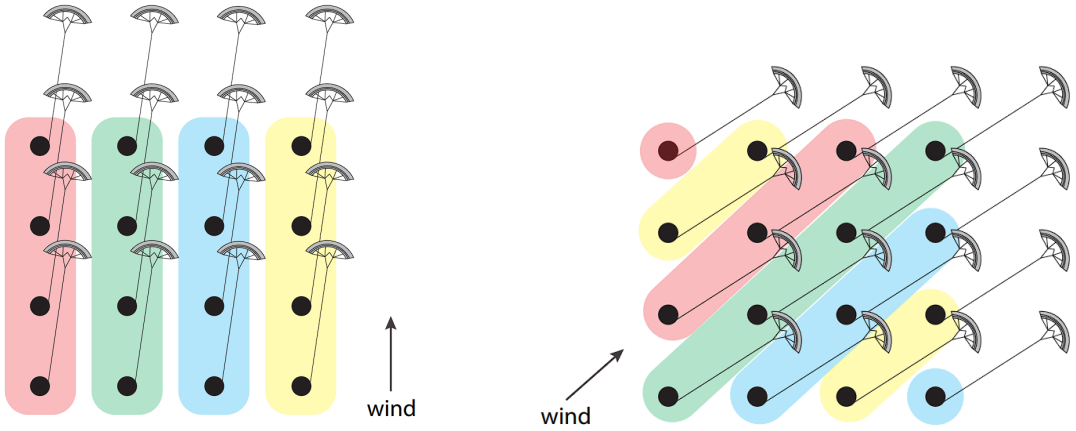

(a) Arrangement for wind from S direction

(b) Arrangement for wind from SW direction

Figure 5.11: Illustration of the arrangement approach proposed by [7].

By aligning the inner and outer columns, the wind farm can achieve a more stable and consistent power output. The phase shift calculation for this modified synchronisation pattern remains straightforward

$$\Theta = \frac{T_c}{n}. \tag{5.9}$$

However, it is important to note that the previously discussed approaches primarily focus on the case of a squared wind farm layout ($n \times n$), which may not always be practical in real-world applications.

When the wind farm layout deviates from a square shape, such as in the case of rectangular or narrow terrain layouts, the outcomes of these approaches can differ significantly. Particularly, when the number of columns greatly differs from the number of rows, the number of groups and phase shifts will vary depending on the wind direction, which can impact the power averaging and stability of the wind farm.

Consider the scenario of a wind farm with a narrow terrain consisting of 4 units arranged in a (4×1) configuration. In this case, when the wind aligns with the direction of the columns, there will be 4 phase shifts corresponding to the 4 groups, each consisting of a single unit. However, the worst-case scenario arises when the wind aligns with the direction of the rows. In this situation, there is only one group, resulting in a single phase shift and no shifting of individual units within the wind farm.

As a result, the deviation of power in the resultant power waveform will be significantly influenced, precisely 4 times the power deviation of a single unit. Figure 5.12 provides a visual representation of this challenging problem.

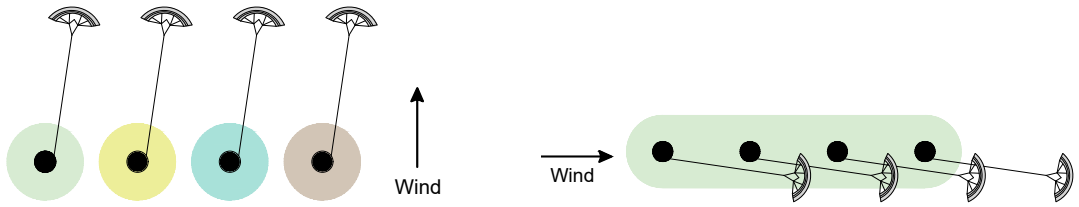

(a) Arrangement for wind from S direction (b) Arrangement for wind from W direction

Figure 5.12: Illustration of one disadvantage of the arrangement in [7].

5.4.2.2 Proposed Approach: Reeling-in within Flight Envelope and Individual Phase Shifts

The proposed approach introduces an innovative operational strategy to tackle the challenges associated with wind farm design. Instead of relying on a significantly higher elevation angle, the approach utilises the maximum elevation angle within a conic-shaped region, as shown in Figure 5.13.

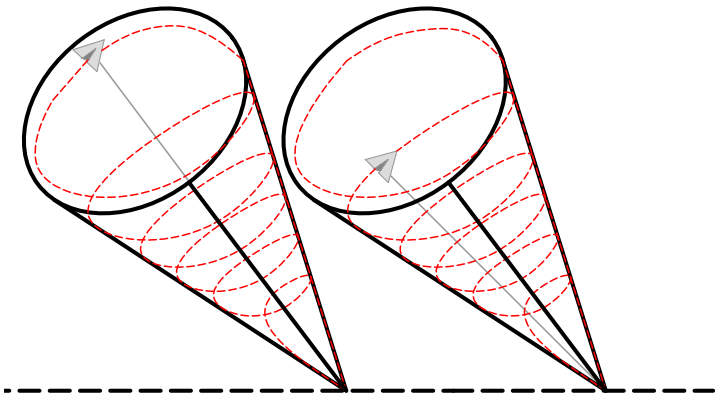

Figure 5.13: Illustration of utilising the retraction elevation angle within the conic-shaped region.

This alternative approach eliminates the need for unit synchronisation, reducing the complexity of control methods required for kite flight control and effectively minimizing the risk of kite collisions during operation.

By adopting this new strategy, each unit within the wind farm operates independently, enabling the implementation of individual phase shifts instead of the previously employed group-based

synchronisation methods. This strategy can be better visualised in Figure 5.14.

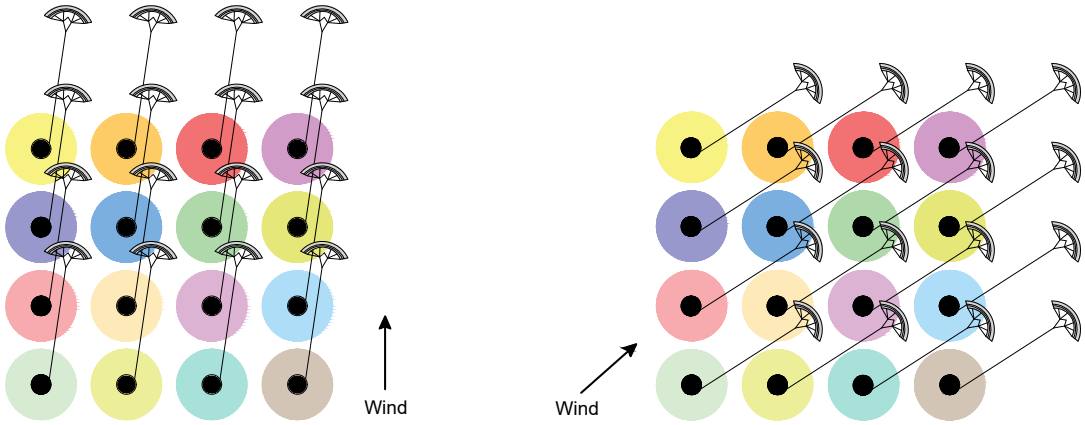

(a) Arrangement for wind from S direction

(b) Arrangement for wind from SW direction

Figure 5.14: Illustration of the proposed arrangement approach.

The phase shift for each unit can be calculated using the following equation

$$\Theta = \frac{T_c}{N_{\text{kites}}}. \tag{5.10}$$

This individual phase shifting leads to significantly reduced deviations in the resultant power waveform of the wind farm, resulting in a smoother and more stable output.

While this approach offers significant advantages, it is crucial to consider its potential drawbacks. One drawback is the possibility of a decrease in the average power output of the wind farm, which can be influenced by the increase in retraction power (P_{re}) associated with the cosine of the retraction angle (β_{re}), as discussed in Equation 4.31. However, this trade-off is accompanied by improved power output levelling, enhancing the stability and integration of the wind farm to the electrical grid.

By levelling the maximum elevation angle and implementing individual phase shifts, this approach demonstrates promising potential in addressing the challenges posed by wind farm design.

5.4.2.3 Complement to the Proposed Approach: Energy Storage Systems (ESS)

To further enhance power output stability, the integration of auxiliary devices like battery energy storage systems (BESS) can be considered. However, the nature of the waveform of the power output of AWES farms, characterised by high power deviations within short time periods and numerous cycles, makes batteries less suitable for this application. The frequent charging and discharging cycles would significantly reduce their lifespan, making them less efficient in addressing this particular challenge. With backup times in hours, response times in seconds, and efficiencies of just 60-80%, batteries are not ideal for this application [41].

A more viable alternative for power smoothing in wind farms is the use of supercapacitors. Supercapacitors offer the advantage of storing electrical energy directly and possess the ability to charge and discharge quickly without compromising efficiency. They can handle high and frequent power demand peaks, making them suitable as a buffer to smooth the power waveform of the wind farm. One of the key characteristics of supercapacitors is their longevity, as they can endure thousands of cycles without significant performance degradation, with a very high efficiency, which exceeds 95% [41].

By integrating supercapacitors into wind farms, power fluctuations can be effectively mitigated, resulting in more stable power output. Supercapacitors offer rapid response times in the millisecond range, making them well-suited for compensating for short-term fluctuations in wind power generation. Furthermore, their longevity and high efficiency make them an attractive option for enhancing the overall performance and reliability of wind farm operations [41].

Further research and development efforts should be focused on optimizing the integration of supercapacitors into wind farm systems, considering factors such as sizing, control strategies, and overall system design. By harnessing the benefits of supercapacitors, wind farms can achieve improved power stability, increased energy utilisation, and enhanced grid integration, contributing to the advancement of this type of renewable energy technology.

Chapter 6

Methodology

In order to obtain solutions for the AWES farms, it is used a BRKGA, which is a type of metaheuristic optimization method. In this chapter, we will provide an overview of the key methodologies used in this study.

We will start by exploring the general approaches employed in the optimization process, highlighting the importance of selecting appropriate methods to tackle complex problems. Next, we focus on Genetic Algorithms (GA), which are powerful computational tools inspired by the principles of natural evolution, and their application in solving optimization problems, as well as their ability to find optimal or near-optimal solutions.

Building upon GA, we introduce the concept of Random Key Genetic Algorithms (RKGA). These algorithms utilise random keys to represent solutions and employ genetic operators to evolve the population towards better solutions. We will examine the fundamental principles behind RKGAs and their suitability for addressing optimization problems.

Furthermore, we will introduce the BRKGA, a variant of RKGA that incorporates bias towards promising solutions, which allows for more efficient exploration of the search space, leading to improved convergence and solution quality. In this section, we will explore the underlying principles and mechanisms of biased random key genetic algorithms, highlighting their relevance in the context of this study.

Finally, we will discuss the application of the BRKGA methodology to the field of AWES to demonstrate the effectiveness and practicality of the BRKGA methodology in this problem of optimization.

6.1 Methods

Optimization problems, which involve finding the best possible solution from a set of feasible options, are encountered across various domains and disciplines. To tackle these problems, two main approaches have been developed: exact methods and approximate methods. These approaches provide different strategies for searching and evaluating potential solutions, each with its own strengths and limitations.

On one hand, algorithms based on exact methods are guaranteed to find the optimal solution to a problem within a finite amount of time. Examples of exact methods include mathematical optimization algorithms such as linear programming, integer programming, and quadratic programming, as well as search algorithms such as depth-first search, breadth-first search, and A* search. These methods can be highly effective, but they may be computationally intensive and may not be practical for problems with numerous variables or constraints [42].

On the other hand, algorithms based on approximate methods are algorithms that do not guarantee finding the optimal solution to a problem but can often find good solutions in a shorter amount of time. These methods are often used for problems that are too complex to be solved exactly or for problems where the optimal solution is not known.

Optimizing power production in a kite farm is a complex problem, and therefore an approximate method may be useful to solve it. Examples of these approximate methods are the metaheuristics, which are a type of approximate method that are characterised by their ability to adapt and learn from the search process, and to explore the solution space more efficiently than traditional optimization methods [42]. Metaheuristics are well-suited to optimization problems with many variables or where the relationships between variables are nonlinear. Some examples of metaheuristic methods include:

1. Particle Swarm Optimization (PSO) is a metaheuristic optimization technique that is based on the behaviour of social animals, such as birds or fish, and their ability to find food or shelter. It involves simulating the movements of a group of particles, each of which represents a potential solution to a problem. The particles update their positions based on their own experience and the experiences of their neighbours, with the goal of finding the optimal solution [43].

2. Ant Colony Optimization (ACO) is an algorithm that is inspired by the foraging behaviour of ants. ACO algorithms use a population of "ants" that communicate with each other using pheromone trails to find good solutions to optimization problems [44]. Each ant represents a possible solution and moves through the solution space by following the pheromone trails left by other ants. The strength of the pheromone trails is determined by the quality of the solutions that they represent, with stronger trails indicating better solutions.

3. Simulated Annealing (SA) is an algorithm that is inspired by the process of annealing in metallurgy, in which a material is slowly cooled to reduce its defects. SA algorithms use a random search process to explore the solution space, but the probability of accepting worse solutions is gradually reduced as the algorithm progresses. This process can be described in metallurgy, where a piece of metal is slowly cooled down, with the aim of finding the optimal solution. The solution is initially generated at a high temperature, which is gradually decreased over time. At each value of temperature, the solution is randomly perturbed to explore new regions of the search space [45].

4. Evolutionary Algorithm (EA) is an algorithm based on the principles of natural selection and genetics. These algorithms work by generating a population of possible solutions, or chromosomes, and applying a selection process to this population by evaluating the fitness of each chromosome based on a predetermined objective function. This function takes into account the performance of the single units under different configurations, as well as any other factors that may be relevant to the optimization problem. EA are used to solve a wide variety of optimization problems, including some that are difficult or impossible to solve using traditional optimization methods. They are well-suited for problems with a large search space, multiple local minima, and noisy or incomplete data [46].

6.2 Genetic Algorithms

Genetic Algorithms (GA) are a specific type of evolutionary algorithm that is based on the principles of natural selection and genetics. These algorithms work by representing potential solutions to a problem as a set of genes or variables and then generating a population of possible solutions, or chromosomes, by randomly assigning values to these genes [47].

In a GA, a population of candidate solutions, chromosomes, is initially generated randomly [47]. These chromosomes are then evaluated based on how well they solve the problem at hand, called the fitness function. In Figure 6.1 the concepts are better described.

The fittest chromosomes are then selected for reproduction, and the process of crossover and mutation is applied to create a new generation of chromosomes. This process is repeated until a satisfactory solution is found or a predefined number of generations have been reached.

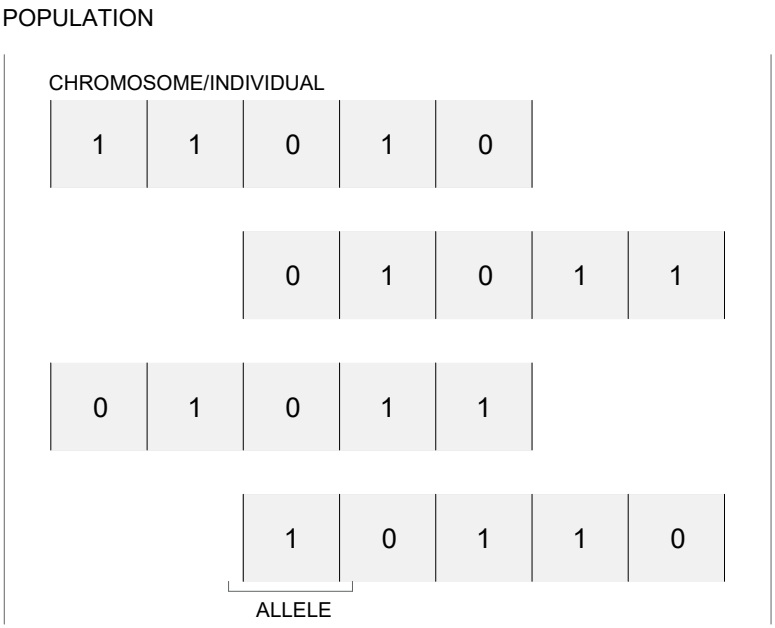

Figure 6.1: Concepts of Genetic Algorithms

Crossover is a vital process in GA that involves the merging of two chromosomes to produce offspring inheriting characteristics from both parents. This procedure introduces diversity into the population and enables GA to explore various regions of the search space. This is accomplished by going through every chromosome and determining whether the child inherits the allele of parent 1 or parent 2. This crossover operation plays a crucial role in optimizing solutions and is widely utilised in genetic algorithms [47].

Mutation is a fundamental component of GA that serves to introduce random changes to the genetic material of a chromosome. Its primary function is to inject diversity into the population in order to prevent the GA from getting stuck in local optima [47]. By randomly selecting specific genes within a chromosome and modifying their values, mutation plays a crucial role in enhancing population diversity and mitigating premature convergence towards suboptimal solutions. While mutation is a crucial mechanism for preventing convergence in local optima, it is important to acknowledge the existence of alternative approaches.

In the specific case being considered, the traditional mutation operation is substituted with the addition of a subset of new individuals to the current population. This strategy aims to broaden the scope of potential solutions, allowing the GA to explore a larger search space and avoid converging towards a local minimum. These new individuals, called mutants, are generated in the same manner as the new population, using randomisation to introduce new solutions. By incorporating this approach, the GA embraces a broader range of possibilities and avoids being overly constrained by the current characteristics of the population.

The introduction of new individuals injects fresh genetic material into the population, fostering exploration in unexplored regions of the solution space. This approach not only enriches the diversity of the population, but also provides the algorithm with a better chance of discovering globally optimal solutions. The algorithm then applies a selection process to this population by evaluating the fitness of each chromosome based on a predetermined objective function [47]. This function takes into account the performance of the genes under different configurations, as well as any other factors that may be relevant to the optimization problem. Elitist strategies include procedures where the chromosomes with the highest fitness are more likely to be selected for reproduction, while those with lower fitness are more likely to be discarded.

Genetic algorithms are well-suited to optimization problems with numerous variables or where the relationships between variables are nonlinear.

6.3 Random Key Genetic Algorithms

RKGA are a variant of genetic algorithms that use a special encoding scheme known as “random keys” to represent the variables or genes in a chromosome. In this encoding scheme, each gene is represented as a continuous value in the interval [0,1] rather than a discrete value, which allows for a more efficient search of the solution space [48].

The algorithm prevents producing unfeasible solutions by guaranteeing a decoder that consistently converts the random-key vector into feasible solutions. As a result of the development

of the population following the Darwinian principle, the fittest people have a better probability of passing on their genetic makeup to next generations. This is accomplished by increasing the probability of reproducing and being copied as elite individuals[48].

As depicted in Figure 6.2, the population of size p is divided into the Elite population (p_e), consisting of the best solutions, and the non-elite group, at the end of each generation. The elite individuals are directly copied to the next generation, implementing an elitism strategy [48]. Additionally, a Mutant population (p_{nkeys}) is generated to introduce diversity by adding random-key vectors. Mutant individuals are randomly generated, similar to the manner in which the individuals are initially created in the population.

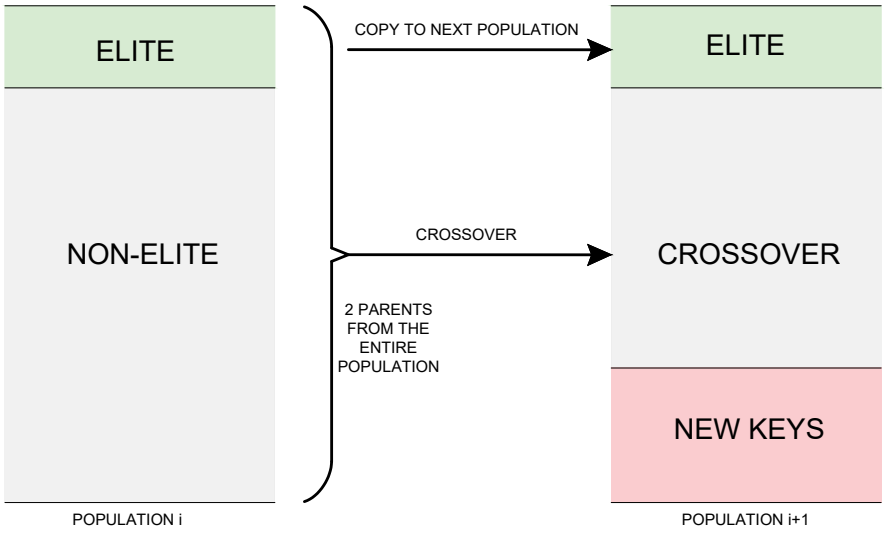

Figure 6.2: Overview of the RKGA

Finally, the remaining $p - p_e - p_{nkeys}$ individuals are generated by combining pairs of randomly selected parents using a uniformly parameterized crossover method. The crossover process involves comparing a random number with the probability of inheriting an allele from the first parent (ρ_a) parameter, which is 50% for RKGA. If the number is less than the percentage, the offspring inherits the allele from the first parent; otherwise, it inherits the allele from the second parent.

The RKGA continues to iterate until a stopping criterion is met, returning the best solution found [48].

6.4 Biased Random Key Genetic Algorithms

BRKGA enhance the search process of RKGA by incorporating bias to improve convergence rate and solution quality while retaining the elitist strategy. In BRKGA, genes in a chromosome are still encoded using random keys, but the algorithm introduces a bias function that directs the search towards regions of the solution space more likely to contain favourable solutions, as illustrated

in Figure 6.3. Specifically, each element in BRKGA is generated by combining one randomly selected element, ensuring that one parent is from the elite group in the current population while the other parent is chosen randomly from the non-elite set of the population [47]. Moreover, biased crossover is employed, increasing the probability of selecting an allele from the chromosome in the elite set.

A key innovation of BRKGA lies in the parent selection for crossover operations. It consistently incorporates one elite parent to cross with one non-elite parent, thereby promoting elitism. Repetition of parents is allowed during the reproduction phase, enabling a parent to have multiple offspring [48].

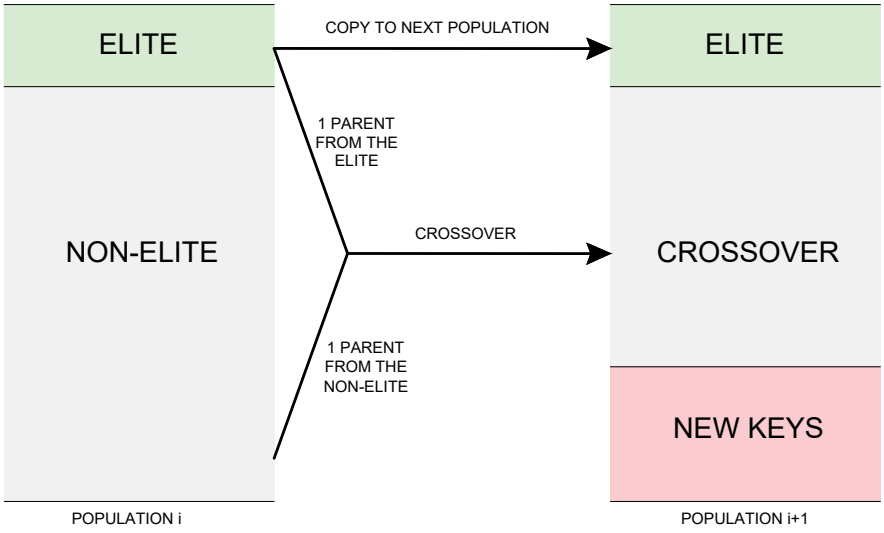

Figure 6.3: Overview of the BRKGA

In terms of crossover, BRKGA introduces a modification, being the probability (ρ_a) of inheriting an allele from the first parent is always set higher than 0.5. As the first parent is always an elite individual, setting $\rho_a > 0.5$ increases the likelihood of offspring inheriting genes from the elite parent, introducing a bias towards elite genes absent in the original RKGA [48]. This procedure can be visualised in Figure 6.4.

Through the iterative process of previous concepts, the BRKGA is employed to optimize the layout of single units in an AWES farm. By adjusting the values of decision variables such as the elevation angle (β), deviation of the elevation angle ($\Delta\beta$), azimuth angle (φ), and maximum tether length ($r_{\max}$), the algorithm aims to converge on a set of optimal solutions. The resulting configurations are then evaluated using computational simulations and experimental testing, as described in [36].

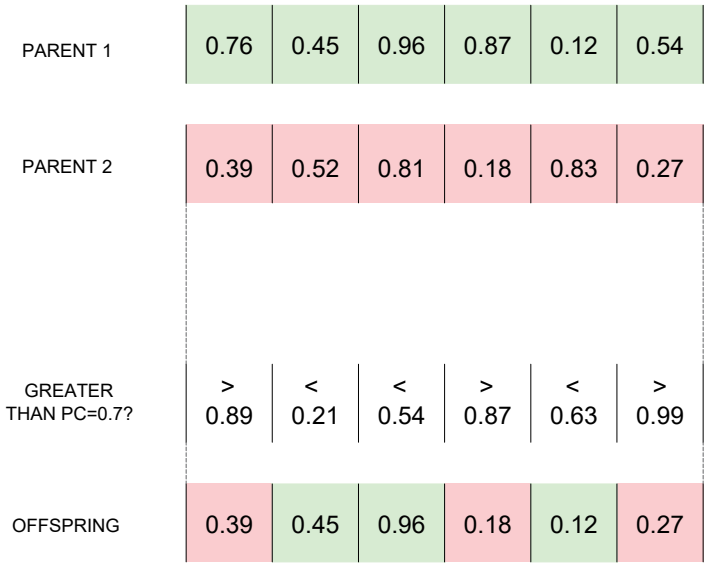

Figure 6.4: Explanation of the biased crossover procedure

6.5 Application to AWES

After this theoretical review, it is important to frame these concepts to the real problem of designing AWES farms.

In this study, the values of the parameters intrinsic to the BRKGA algorithm are presented in the following Table 6.1.

Table 6.1: Parameters in the BRKGA

Parameter	Value
Percentage of elite population (ρ_e)	20%
Percentage of population from crossover (ρ_{cross})	50%
Percentage of new keys population (ρ_{nkeys})	30%
Crossover biased parameter (ρ_a)	0.7

As seen, this means that 20% of the population will be denoted as an elite part of the population and therefore those chromosomes will be copied to the next generation, and 30% of the population will be created by the new keys, generated by randomness when deciding the values of the alleles. Lastly, the ρ_a as 0.7 means that there is a bias regarding the decision of parent choice, as used in BRKGA.

To illustrate the implementation of the algorithm, a flowchart is provided in Figure 6.5, showcasing the step-by-step process of the BRKGA in optimizing the unit locations within the AWES.

In the specific case at hand, the output of the algorithm includes power analysis measurements, such as average production, power density, and annual energy production. Initially, the algorithm is executed a first time to determine the maximum number of kites that can fit within the designated kite farm for optimal wind speed characteristics.

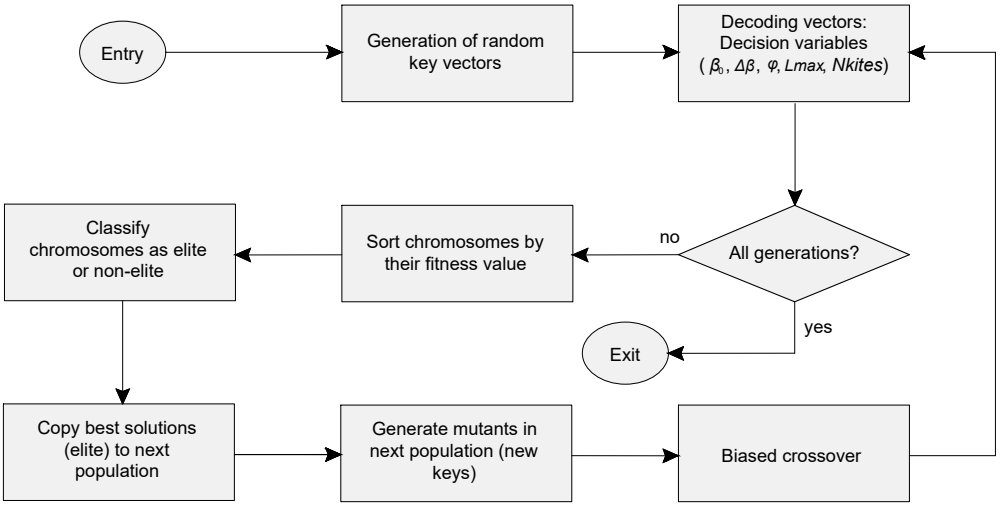

Figure 6.5: Flowchart of the process of the BRKGA [8]

Subsequently, the BRKGA process is repeated with the constraint of power limitation based on the nominal power of the studied model, where the number of kites is already determined from the previous run. This iterative process is visually represented in the provided flowchart, as seen in Figure 6.6.

It is worth noting that by employing penalty mechanisms, the algorithm effectively discourages unfeasible solutions. For instance, solutions that exhibit excessively high roll angles are penalized to prevent the kites from operating within a confined area. This ensures that the kite wind farm configuration does not consist of numerous units occupying a disproportionately small space.

The iterative nature of the algorithm, combined with the incorporation of power limitations and penalty mechanisms, allows for the exploration of feasible solutions and the identification of optimal configurations for the AWES.

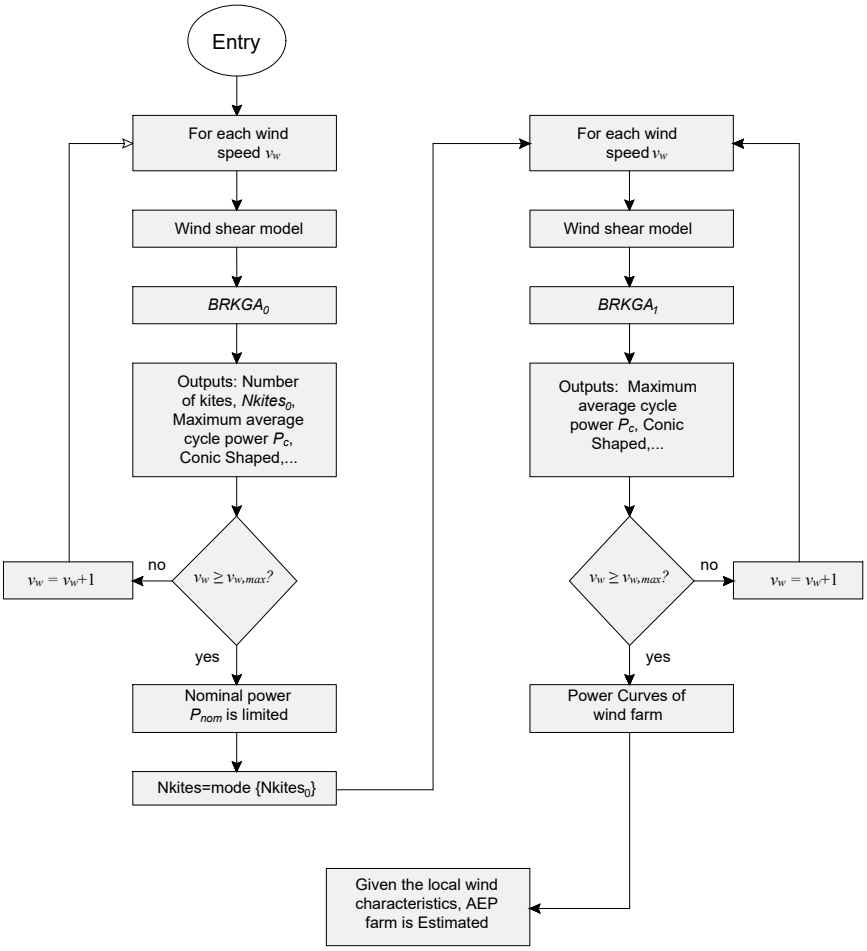

Figure 6.6: Flowchart of the implemented algorithm [8]

Chapter 7

Case Study

This chapter presents a case study for a real application where we apply the theoretical concepts discussed in the previous chapters. We begin by characterising the site and assessing the wind resource at the chosen location. Subsequently, we analyse the power output and explore various measurements that are relevant to the evaluation of the feasibility of the implementation of the kite wind farm, as well as approach several constraints inherent from them such as the power averaging of the wind farm.

7.1 Site Characterisation and Resource Assessment

In this case study, we focus on a specific location chosen for the kite wind farm project. The site selected is located in Montalegre, Portugal, where the terrain offers a suitable location for studying wind energy due to its geographical features and wind patterns. The terrain can be visualised in the following Figure 7.1.

It is worth emphasising that this study relies on certain assumptions regarding the characteristics of the terrain. These assumptions include considering the terrain as a rectangular shape with specified dimensions, which establishes a simplified representation of the area in order for easier analysis and assessment of the kite wind farm design. These dimensions are summarised in Table 7.1 to provide a clear understanding of the specifications of the terrain. It should be noted that the terrain is oriented longitudinally to the North direction.

By assuming a rectangular shape for the terrain, the study establishes a simplified representation of the area under consideration.

Table 7.1: Terrain specifications in the case study

Terrain		
Parameter	Value	Unit
Cut-in Speed	3	$\mathrm{m\,s^{-1}}$
Cut-out Speed	18	$\mathrm{m\,s^{-1}}$
L_{Land}	800	m
W_{Land}	600	m

Figure 7.1: Overview of the location of the case study

The provided table outlines the specific characteristics of the terrain considered in the case study. By incorporating these terrain parameters into the analysis, we can assess the suitability and potential challenges associated with implementing an AWES in this particular area.

7.1.1 Data Gathering and Estimation

On site, a measuring tower is also installed to collect relevant information about the site where the units are to be installed. This is normally installed a few years before the installation of the farm, so that a site characterisation study can be carried out, where the data collected allows us to understand how the farm energy production will be and the viability of the installation, generally being the starting point of the project.

However, the measuring tower is unable to directly measure the wind speed at the altitudes where the AWES will operate. Consequently, the wind speeds at these higher altitudes need to be estimated using the information obtained from the wind shear analysis discussed in Section 4.1.1.

In this project, wind measurements were conducted at heights of 45 and 85 meters and were collected with a timestamp of 10 minutes for the entire year of 2022. By applying the least squares minimization method, reviewed in Section 4.1.1, we determined the terrain roughness (z_0) that best fits the measured data. It is important to highlight that this calculation was performed for each wind direction, divided into sectors.

For the purpose of this study, we divided the wind directions into 12 groups, with each group differing by 30°, as seen in the Table 7.2, where it is possible to visualise the values of the terrain roughness calculated.

Table 7.2: Division of sectors

Sector	from (°)	to (°)	z_0
1	345	15	0.0102
2	15	45	0.0778
3	45	75	0.1509
4	75	105	0.1542
5	195	135	0.1701
6	135	165	0.3321
7	165	195	0.2518
8	195	225	0.0731
9	225	255	0.1181
10	255	285	0.0719
11	285	315	0.2136
12	315	345	0.2908

7.1.2 Frequency and Speed

Determining the prevailing wind direction is crucial for optimizing the operation and maximizing the energy production of an AWES. By analysing wind frequency and speed in different sectors at a specific altitude, such as 150 meters, we can gain valuable insights regarding the predominant wind origins distribution of wind speeds.

To comprehensively assess the wind resource, it is essential to consider both wind frequency and wind speed in each direction. The analysis of wind frequency provides information about the occurrence of wind from different directions, while the evaluation of wind speed quantifies the energy potential available in each direction. Figure 7.2 illustrates the wind frequency and speed for each direction.

The analysis reveals a predominance of wind coming from the West, indicating that this direction serves as the primary source of wind for this location. On the other hand, the wind frequency from the North and South directions is relatively lower.

When examining the wind speed data, it becomes apparent that most directions maintain relatively consistent wind speeds. However, the North and South directions exhibit lower wind speeds compared to the other sectors.

These findings underscore the importance of considering both wind frequency and wind speed in the evaluation of wind resource. While wind frequency insights provide an understanding of the occurrence of wind from various directions, wind speed measurements are crucial for assessing the energy potential that can be harnessed by AWES.

7.1.3 Weibull Distribution

Following the analysis, we proceeded to conduct the Weibull distribution for each velocity interval, utilising the methodology described earlier in Section 4.1.3. By fitting the Weibull distribution to the wind speed data, we can obtain a probability density function that describes the likelihood of different wind speeds occurring.

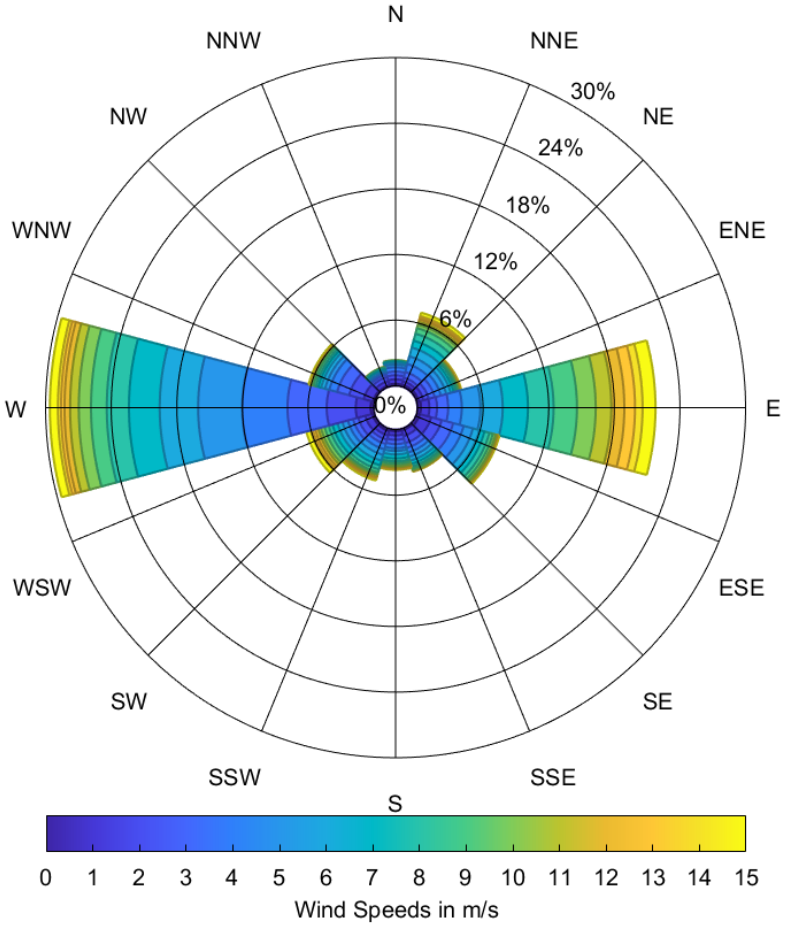

Figure 7.2: Illustration of wind speed and frequency by sectors

The resulting graphs in Figure 7.3 illustrate the Weibull distribution for each velocity interval, depicting the probability density function for the corresponding wind speed range.

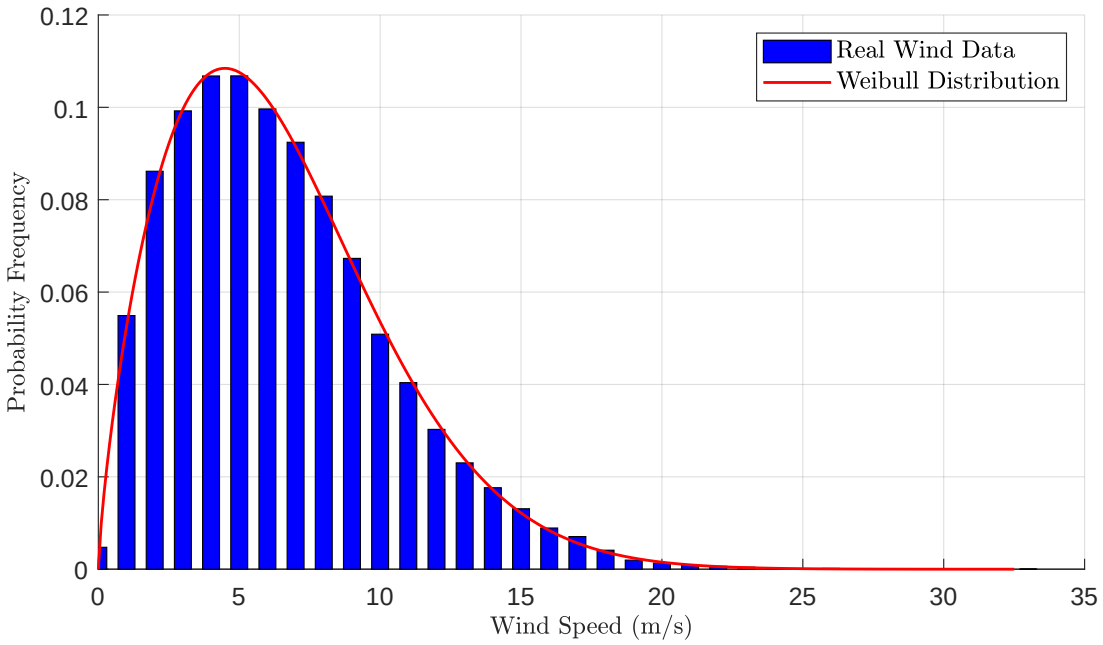

Figure 7.3: Weibull distribution for the case study

After analysing the histograms, we can observe a close approximation between the Weibull distribution and the frequency distribution. The Weibull distribution displays a scale value of 7.30 m/s, which represents the average wind speed within the specified velocity intervals. Additionally, the shape parameter calculated is 1.75, indicating the variability and shape of the distribution.

The strong correspondence between the Weibull distribution and the frequency distribution implies that the Weibull model accurately captures the wind speed characteristics, which is vital, as this alignment enables precise predictions and estimations regarding the wind resource.

7.2 Analysis

To perform precise calculations about power production, it is crucial to have detailed knowledge of the specifications and technical parameters of the AWES units. For this study, the AWES unit utilised was based on the small-scale prototype employed in the UPWIND Project. Table 7.3 provides an overview of the key information regarding the unit used.

7.2.1 Layout

Determining the optimal layout for a kite wind farm is crucial for maximizing power output. In this case study, we compare the squared and hexagonal layouts to identify the better option. The

Table 7.3: Single unit specifications in the case study

AWES unit		
Parameter	Value	Unit
P_{nom}	1500	W
c_L	1.7	
c_D	0.17	
A	0.28	m^2
m	0.7	kg
$L_{\min}$	50	m
$L_{\max}$	250	m

terrain dimensions are known, thus necessitating an analysis to determine the most suitable layout.

To evaluate the performance of the layouts, the starting point is to compare the individual performance of the single units that compose the layouts. This can be visualised in the following Figure 7.4.

The power curve for the squared layout shows slightly higher power generation across various wind speeds. However, the hexagonal layout offers an advantage in terms of unit placement. The smaller area occupied by each unit allows for the placement of 45 units within the terrain, while the squared layout accommodates only 35 units.

Figure 7.5 illustrates the arrangement of units for each layout. Figure 7.5(a) depicts the squared layout with 35 units, while Figure 7.5(b) shows the hexagonal layout with 45 units.

Considering the difference in unit quantities, we can compare the overall power output of the kite wind farm. The power curves for the wind farm can be visualised in Figure 7.6.

From Figure 7.6, it is possible to verify the hexagonal layout presents a higher power production compared to the squared layout. To compare both layouts from another point of view, other power measurements for each layout are presented in Table 7.4. It is possible to see more information about the results in Appendix A.

Table 7.4: Comparison of power measurements between layouts

Power Measurements					
Layout	P_{avg} (kW)	AEP (MWh)	PD $\left(\mathrm{W\,m^{-2}}\right)$	CF	$\mathrm{Hours_{eq}}$(h)
Squared	17.7	155.4	0.0370	0.3967	3475
Hexagonal	20.4	178.7	0.0425	0.3547	3107

The hexagonal layout exhibits an average power output of 20.4 kW, which is significantly higher than the average power output of 17.7 kW for the squared layout.

In terms of AEP, the hexagonal layout produces 178.7 MWh, whereas the squared layout generates 155.4 MWh. This substantial difference indicates that the hexagonal layout is capable of harnessing a larger amount of wind energy over a year.

When considering power density, which measures the power generated per unit area, the

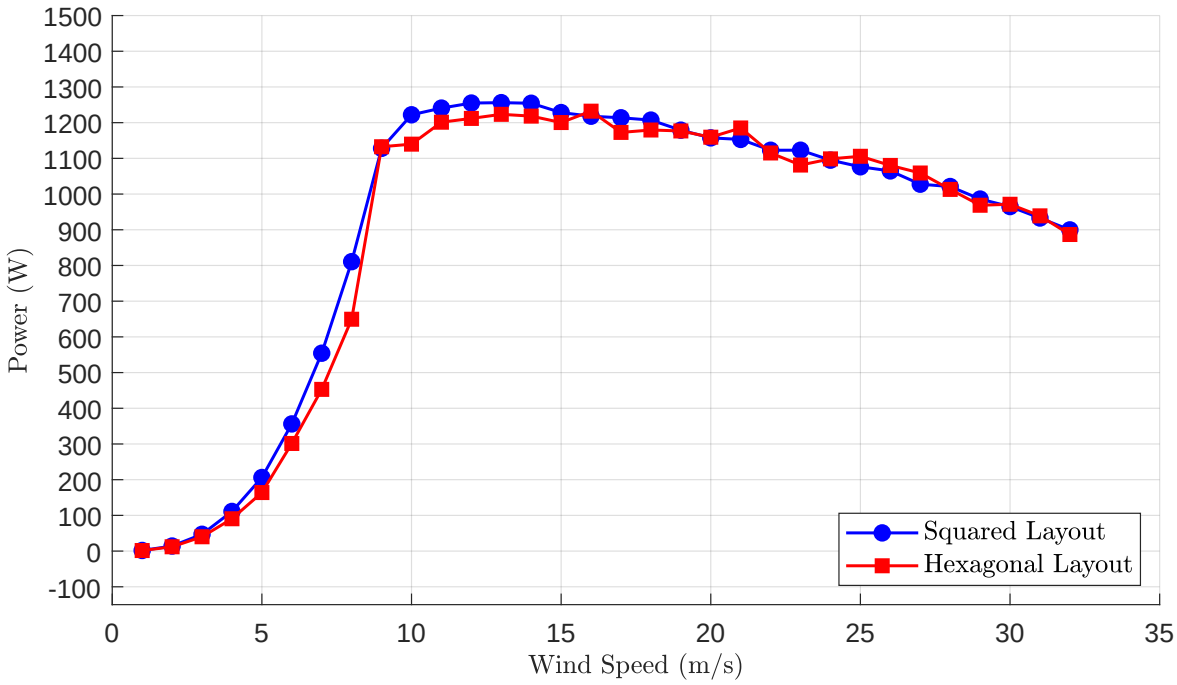

Figure 7.4: Unit ACP for both layouts

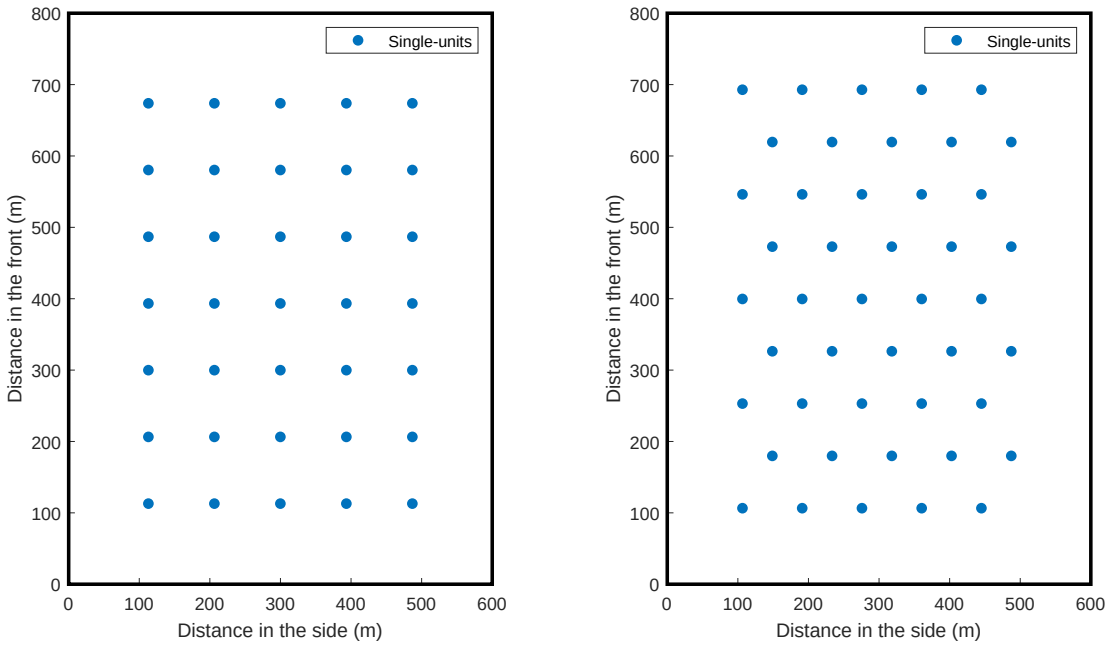

(a) Squared layout (35 units)

(b) Hexagonal layout (45 units)

Figure 7.5: Different types of layout

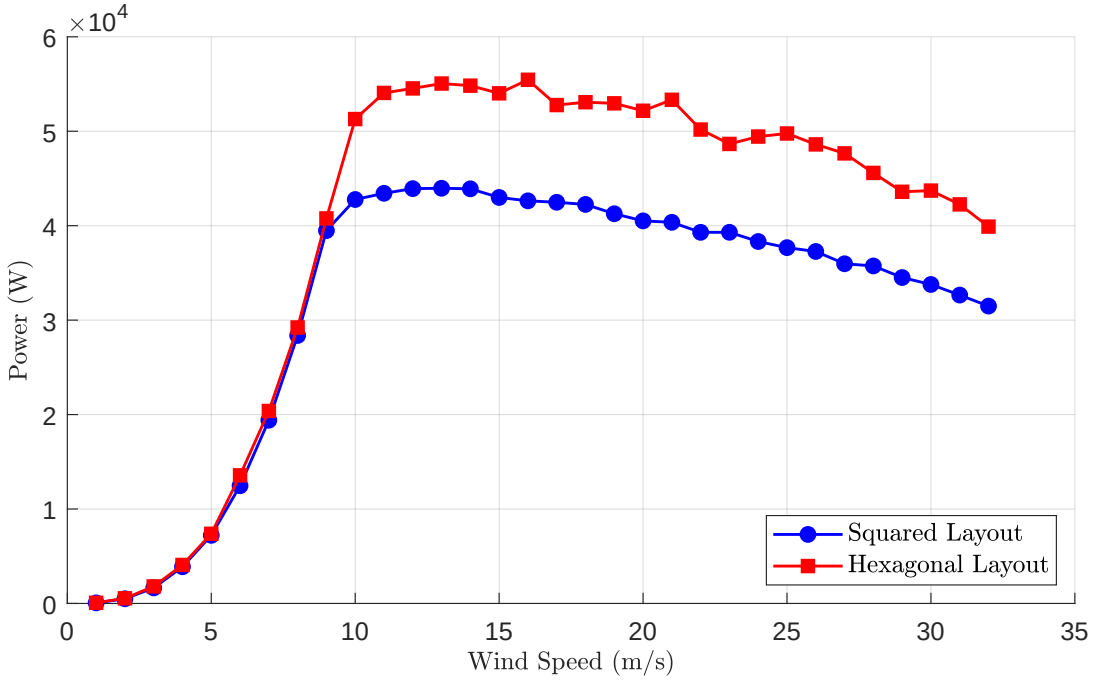

Figure 7.6: Wind farm ACP for both layouts

hexagonal layout achieves a value of 0.0425 $\mathrm{W\,m^{-2}}$, while the squared layout has a power density of 0.0370 $\mathrm{W\,m^{-2}}$. This suggests that the hexagonal layout is more effective in utilising the available land area, resulting in more concentrated power output.

However, the squared layout demonstrates a better capacity factor of 0.3967 compared to the capacity factor of the hexagonal layout of 0.3547. The capacity factor represents the actual power generated relative to the maximum potential power. A higher capacity factor indicates that the squared layout operates closer to its nominal capacity, taking better advantage of the available wind resource.

Furthermore, the equivalent hours for the squared layout are 3475 h, while the hexagonal layout requires 3107 hours. Equivalent hours represent the number of hours at the nominal capacity needed to produce the same energy output as the actual situation. This implies that the squared layout operates at its nominal capacity for a longer duration compared to the hexagonal layout.

Taking all these factors into consideration, it can be concluded that the hexagonal layout offers a significant advantage in terms of average power output and AEP. Its higher power density also suggests a more efficient use of the available land area. However, the squared layout exhibits better performance in terms of capacity factor and equivalent hours, indicating that each unit operates closer to its full capacity.

After conducting the analysis, it can be concluded that the hexagonal layout provides advantages in terms of overall power production for the kite wind farm. The arrangement of units in a hexagonal pattern allows for better utilisation of the available wind resources. On the other hand, the square layout proves beneficial for enhancing the power production of individual units.

7.2.2 Power Averaging

In addition to analysing the average power output, it is crucial to consider the stability of the power output. When connecting a wind farm to the grid, it is important for the power output to be as consistent as possible. Variations in power output can cause instability and difficulties in grid integration, affecting system reliability. To address this aspect, we will perform a power averaging analysis and compare proposed approaches to improve power stability.

For this analysis, we will focus on a specific period when the wind speed remains constant. As determined in the previous section, we will continue using the hexagonal layout, which allows for the placement of 45 units within the terrain for both approaches under study.

The first approach, reviewed in Section 5.4.2.1, involves an operational strategy where the retraction phase of the AWES occurs out of the conic-shaped region. This particular configuration requires precise synchronisation of aligned units to avoid collisions during operation, as any deviation or inconsistency in the retraction timing could lead to potential collisions. In the first approach, with the hexagonal layout, there are 45 units distributed in the terrain. When the wind predominantly comes from the west direction, the units form 9 groups, each with a phase shift of $\Theta = T_c/9$, where T_c represents the period of the wind cycle.

In contrast, the second approach, proposed in Section 5.4.2.2, introduces a solution that retracts the kite at the verge of the conic-shaped region. This layout design allows the single units to operate independently, as the conic-shaped regions are guaranteed not to intersect. By eliminating the need for strict synchronisation, the second approach offers greater flexibility and reduces the risks associated with collisions. Considering the terrain, as well as the layout, this approach proposes a layout with 45 phase shifts, corresponding to the 45 units in the kite wind farm for every wind direction. This means that the phase shift will be $\Theta = T_c/45$, significantly reducing its magnitude. The following Figure 7.7 illustrates the groups and phase shifts for the predominant wind direction for both approaches.

By comparing the two approaches, it becomes clear that the resultant waveform of the first approach, with groups composed of 5 units, exhibits larger deviations. This leads to poorer stability and more significant complications when connecting to the grid. Figure 7.8 shows the resultant waveforms of both approaches. The peaks in the waveform of the first approach are much more prominent due to the groups composed of 5 units.

These waveforms represent the steady state of the power output when the wind predominantly comes from the studied direction. In Table 7.5, it is possible to compare the measurements between both approaches.

Table 7.5: Comparison of power measurements between approaches

Power Measurements			
Approach	P_{avg} (kW)	Θ (s)	ΔP (kW)
β_{out}	52.571	0.3967	8.012
β_{in}	52.466	0.3547	1.627

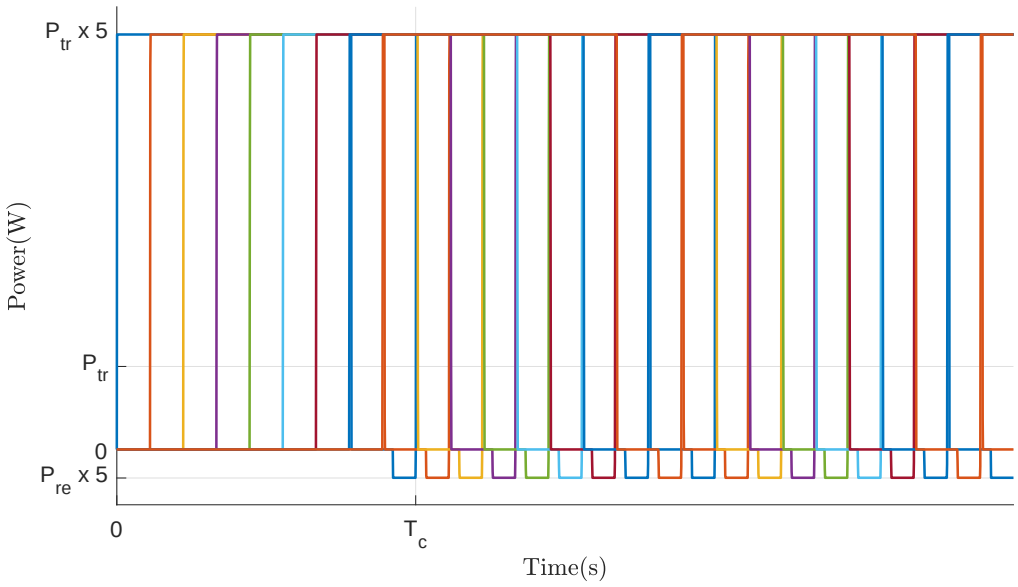

(a) β_{out} (9 groups)

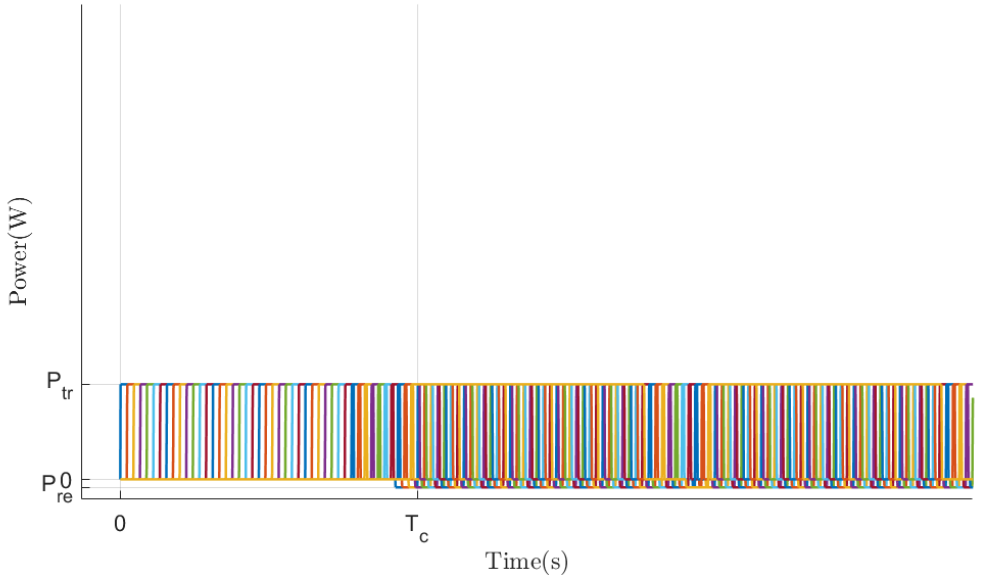

(b) β_{in} (45 groups)

Figure 7.7: Phase shifts for the different approaches

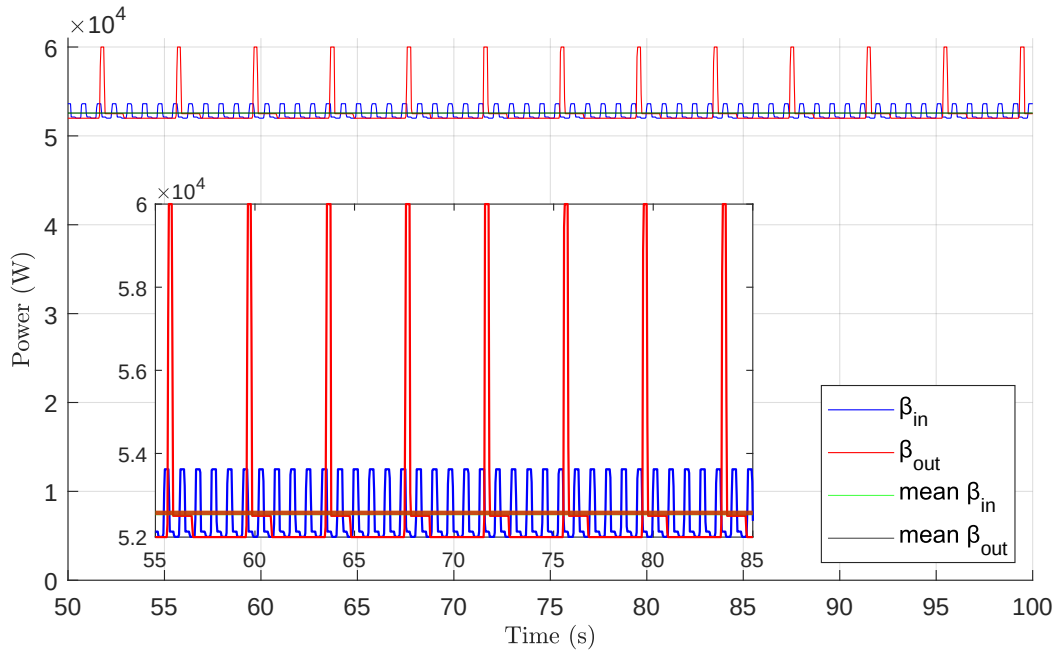

Figure 7.8: Resultant Waveform for the different approaches

Upon reviewing the data presented in the previous table, it is evident that both approaches yield similar average power outputs within the given timeframe, with a slightly higher average power output in the first approach of 0.2%. However, there is a notable distinction in the power deviation over time between the two approaches. The synchronised units within groups approach exhibits a higher power deviation characterised by frequent peaks, while the second approach demonstrates a more stable power output with lower magnitude peaks. The frequent peaks can strain the grid infrastructure. In contrast, the second approach offers a more favourable power output with reduced peak magnitudes, facilitating smoother integration with the grid.

To mitigate the power deviation seen in the waveforms, future improvements can be made by implementing auxiliary devices, as discussed in Section 5.4.2.3. For the new approach, with smaller deviations, it would be easier to implement a solution such as a supercapacitor, which possesses the necessary characteristics to handle the nature of these waveforms. However, mitigating the deviation in the first approach would be more challenging, as the deviation is much larger, making it difficult to store that magnitude of energy for a small amount of time.

In conclusion, the power averaging analysis demonstrates that the new approach offers better power stability compared to the first approach. Although the average power output is slightly lower, the smaller deviation in power makes it a more suitable option for grid integration.

Future advancements in auxiliary devices, such as supercapacitors, can further enhance power stability in the new approach.

Chapter 8

Conclusions and Future Work

In this study, we have developed an optimization algorithm that aims to maximize the power production of a kite wind farm. The algorithm focuses on optimizing the flight envelopes of individual units while considering the constraints imposed by the specific terrain characteristics. In our study, the terrain characteristics were derived from real data, ensuring the practical relevance of this work.

The BRKGA is well-suited for addressing this type of problem because of its ability to efficiently explore a large solution space and to discover solutions to flight envelopes of individual units in order to study various AWE farm layouts, resulting in improved power production results.

Moreover, the preceding analysis of wind conducted in the case study proved to be crucial in the context of wind farm optimization. Understanding the wind patterns and speeds enables a better selection of appropriate flight envelopes and placement of units. This information is vital for maximizing energy production while ensuring the stability and safety of the kite farm.

Additionally, the wind shear model played a critical role in accurately estimating the wind behaviour at different altitudes. By integrating the wind shear model into the BRKGA, it accounts for the variation of wind speed along the height, which is significant for optimizing the kite flight configurations and maximizing power production. Through the incorporation of the wind shear model, our algorithm achieves a more realistic representation of wind characteristics, leading to more reliable and effective kite farm layouts.

Two different layout patterns, namely square and hexagonal, were investigated to determine which layout would yield the highest energy production in the given scenario. Firstly, the square layout promotes superior performance for individual units, since it operates within a larger flight envelope and closer to their nominal power output. Secondly, the hexagonal layout proves to be advantageous for the overall power production of the wind farm, since being the densest arrangement, facilitates the placement of a larger number of units within the same terrain dimensions. This increased density results in higher total power production for the wind farm as a whole.

In addition to optimizing the power production of the wind farm, this study also addressed the challenge of power averaging to facilitate grid connection and enhance the feasibility of wind farms in practical applications. Two different approaches were investigated to mitigate the power

deviation issue during the retraction phase of the kite. One approach involved the need for synchronising units within each group to prevent collisions that may occur when a kite comes out of its flight envelope for the retraction phase. While this approach presents just a slightly higher power average, it requires the implementation of control strategies and reduces the flexibility of the system in real-world applications. In contrast, the proposed alternative approach aimed to achieve a more stable and consistent power output from the wind farm. Although there was a minor decrease in the overall power produced, this approach yields significant benefits in terms of average power deviation, as the variations over time are substantially reduced. As a result, the wind farm exhibits a more constant and predictable power output, which greatly facilitates grid integration. Having a more stable power output, the strain on the grid infrastructure is reduced, and it enables easier integration with other sources of energy.

These contributions promote the advancement of wind farm technology by providing insights into the optimization between power production and grid integration. By adopting approaches for power output maximization and power stability, wind farms can become more efficient, reliable, and seamlessly integrated into existing electrical grids. This research paves the way for future studies and practical implementations of wind farms, fostering the widespread adoption of clean and sustainable energy sources.

In the future, there is a potential for further exploration and optimization of wind farms, particularly in terms of designing new layouts which optimize distances between kites and the ground area covered by each unit. Currently, the spacing between units is typically determined based on radial distances, as it is defined as a circular ground area around the unit. However, future studies should investigate the use of ellipses to define the ground area covered by each unit and eventually other geometrical shapes to define the distance between units. By optimizing the ground area allocated to each unit according to wind characteristics, it may be possible to reduce the distances between kites, potentially increasing the overall power density of the wind farm. This trade-off between unit production and the number of units employed would need to be carefully evaluated, taking into account the LCOE to ensure economic viability.

Additionally, for enhanced grid stability and integration, the application of ESS can be explored. By storing excess energy during peak production periods and discharging it during low production periods, ESS can help smooth out the power waveform and ensure a more consistent and reliable power output. The selection and implementation of appropriate ESS technologies and control strategies would be essential to optimize the performance and efficiency of wind farms.

Appendix A

Complementary Results

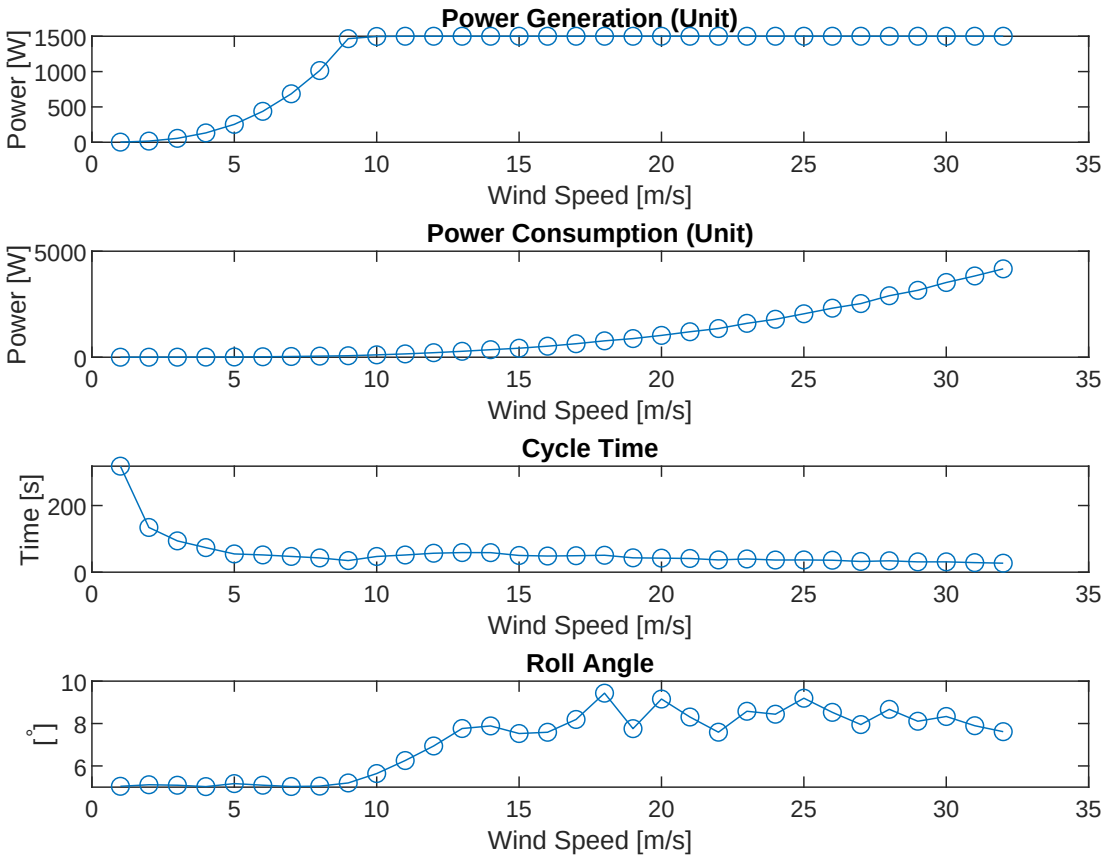

Figure A.1: Square layout results

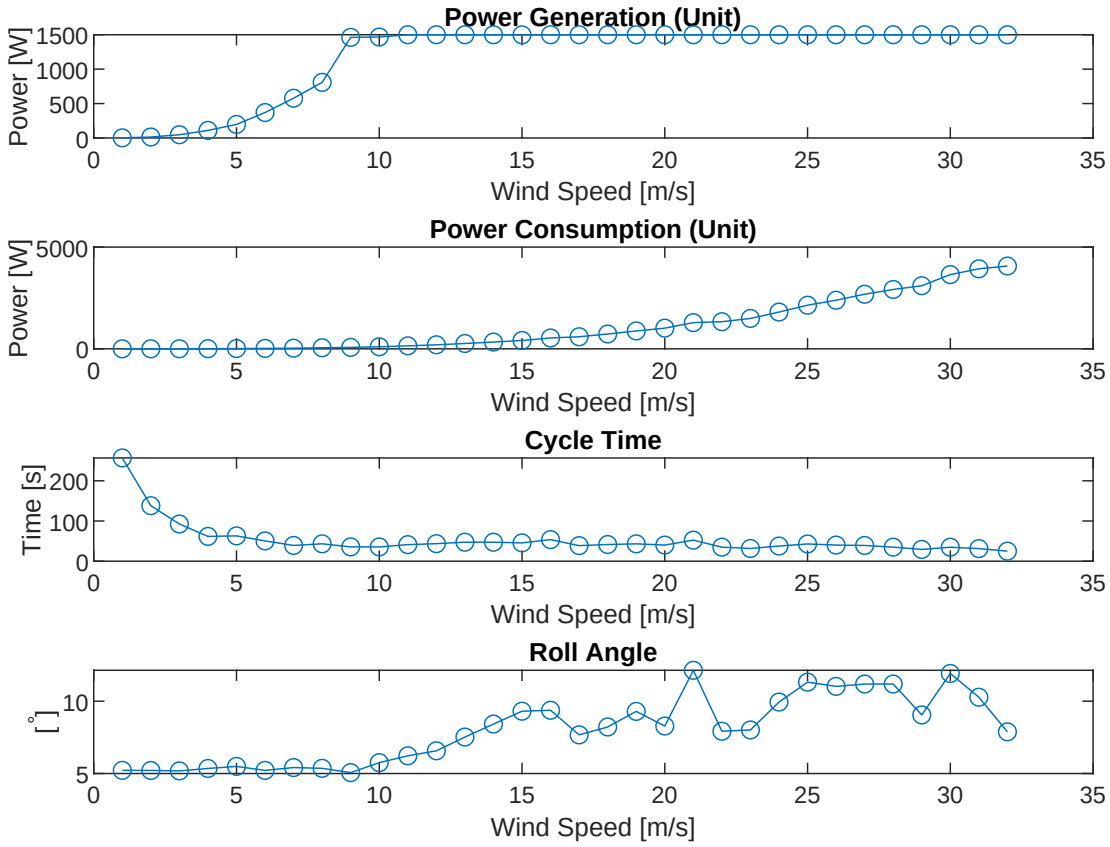

Figure A.2: Hexagonal layout results

References

[1] Hannah Ritchie, Max Roser, and Pablo Rosado. Energy. URL: https://ourworldindata.org/energy.

[2] Sector by sector: where do global greenhouse gas emissions come from? URL: https://ourworldindata.org/ghg-emissions-by-sector.

[3] Jochem Weber, Melinda Marquis, Aubryn Cooperman, Caroline Draxl, Rob Hammond, Jason Jonkman, Alexsandra Lemke, Anthony Lopez, Rafael Mudafort, Mike Optis, Owen Roberts, and Matt Shields. Airborne Wind Energy. *Renewable Energy*, 2021.

[4] UP WIND Project. URL: http://www.upwind.pt.

[5] Manuel Fernandes, Sérgio Vinha, Luís Paiva, and Fernando Fontes. L0 and L1 Guidance and Path-Following Control for Airborne Wind Energy Systems. *Energies*, 15:1390, February 2022. doi:10.3390/en15041390.

[6] Delft University of Technology. Airborne Wind Energy Conference 2021 (AWEC 2021). 2022. Publisher: Delft University of Technology. URL: http://resolver.tudelft.nl/uuid:696eb599-ab9a-4593-aedc-738eb14a90b3, doi:10.4233/UUID:696EB599-AB9A-4593-AEDC-738EB14A90B3.

[7] Manuel Côrte-Real de Matos Fernandes. Airborne wind energy systems: Modelling, simulation and economic analysis. 2018.

[8] Luís A. C. Roque, Manuel C. R. M. Fernandes, Luís Tiago Paiva, and Fernando A. C. C. Fontes. Optimal layout in airborne wind energy farms. 2023. URL: https://zenodo.org/record/8095966, doi:10.5281/zenodo.8095966.

[9] Hannah Ritchie, Max Roser, and Pablo Rosado. Energy. *Our World in Data*, 2022. URL: https://ourworldindata.org/energy.

[10] Mark Z. Jacobson and Mark A. Delucchi. Providing all global energy with wind, water, and solar power, Part I: Technologies, energy resources, quantities and areas of infrastructure, and materials. *Energy Policy*, 39(3):1154–1169, March 2011. URL: https://www.sciencedirect.com/science/article/pii/S0301421510008645, doi:10.1016/j.enpol.2010.11.040.

[11] Dr Fatih Birol. World Energy Outlook 2022.

[12] Dr Fatih Birol. World Energy Outlook 2019.

[13] About the secretariat | UNFCCC. URL: https://unfccc.int/about-us/about-the-secretariat.

[14] The Paris Agreement | UNFCCC. URL: https://unfccc.int/process-and-meetings/the-paris-agreement.

[15] United Nations. THE 17 GOALS | Sustainable Development, 2015. URL: https://sdgs.un.org/goals.

[16] Wind Energy Basics. URL: https://www.energy.gov/eere/wind/wind-energy-basics.

[17] André F. C. Pereira and João M. M. Sousa. A Review on Crosswind Airborne Wind Energy Systems: Key Factors for a Design Choice. *Energies*, 16(1), 2023. URL: https://www.mdpi.com/1996-1073/16/1/351, doi:10.3390/en16010351.

[18] Zeashan H. Khan and Muhammad Rehan. Harnessing Airborne Wind Energy: Prospects and Challenges. *Journal of Control, Automation and Electrical Systems*, 27, July 2016. doi:10.1007/s40313-016-0258-y.

[19] Antonello Cherubini. *Advances in airborne wind energy and wind drones*. Scuola Superiore Sant'Anna, 2017.

[20] Antonello Cherubini, Andrea Papini, Rocco Vertechy, and Marco Fontana. Airborne Wind Energy Systems: A review of the technologies. *Renewable and Sustainable Energy Reviews*, 51:1461–1476, November 2015. URL: https://www.sciencedirect.com/science/article/pii/S1364032115007005, doi:10.1016/j.rser.2015.07.053.

[21] Bruce Valpy Mike Blanch, Alexi Makris. Getting airborne – the need to realise the benefits of airborne wind energy for net zero, bvg associates on behalf of airborne wind europe, september 2022.

[22] Miles L. Loyd. Crosswind kite power (for large-scale wind power production). *Journal of Energy*, 4(3):106–111, May 1980. Publisher: American Institute of Aeronautics and Astronautics. URL: https://arc.aiaa.org/doi/10.2514/3.48021, doi:10.2514/3.48021.

[23] Chris Vermillion, Mitchell Cobb, Lorenzo Fagiano, Rachel Leuthold, Moritz Diehl, Roy S. Smith, Tony A. Wood, Sebastian Rapp, Roland Schmehl, David Olinger, and Michael Demetriou. Electricity in the air: Insights from two decades of advanced control research and experimental flight testing of airborne wind energy systems. *Annual Reviews in Control*, 52:330–357, January 2021. URL: https://www.sciencedirect.com/science/article/pii/S1367578821000109, doi:10.1016/j.arcontrol.2021.03.002.

[24] Makani. URL: https://x.company/projects/makani/.

[25] R. Katebi, J. Samson, and C. Vermillion. A Critical Assessment of Airborne Wind Energy Systems. In *2nd IET Renewable Power Generation Conference (RPG 2013)*, pages 3.46–3.46, Beijing, China, 2013. Institution of Engineering and Technology.

[26] Skysails. URL: https://skysails-power.com/about-us/.

[27] Kite power for mauritius. URL: https://skysails-power.com/kite-power-for-mauritius/.

[28] Kitepower - Airborne Wind Energy. URL: https://thekitepower.com/.

[29] Omnidea. URL: https://www.omnidea.net/aerial-platforms.html.

[30] Martin O. L. Hansen. *Aerodynamics of wind turbines*. Earthscan, London ; Sterling, VA, 2nd ed edition, 2008.

[31] Steven J Miller. The Method of Least Squares. 2006.

[32] Waloddi Weibull. A statistical distribution function of wide applicability. *Journal of applied mechanics*, 1951.

[33] Isaac Y. F Lun and Joseph C Lam. A study of Weibull parameters using long-term wind observations. *Renewable Energy*, 20(2):145–153, June 2000. URL: https://www.sciencedirect.com/science/article/pii/S0960148199001032, doi:10.1016/S0960-1481(99)00103-2.

[34] Rolf Luchsinger, Damian Aregger, Florian Bezard, Dino Costa, Cédric Galliot, Flavio Gohl, Jannis Heilmann, Henrik Hesse, Corey Houle, Tony Wood, and Roy Smith. Pumping Cycle Kite Power with Twings. In *Green Energy and Technology*, pages 603–621. April 2018. Journal Abbreviation: Green Energy and Technology. doi:10.1007/978-981-10-1947-0_24.

[35] Roland Schmehl, Uwe Ahrens, and Moritz Diehl. *Airborne Wind Energy*. November 2013. doi:10.1007/978-3-642-39965-7.

[36] Luís A. C. Roque, Luís Tiago Paiva, Manuel C. R. M. Fernandes, Dalila B. M. M. Fontes, and Fernando A. C. C. Fontes. Layout optimization of an airborne wind energy farm for maximum power generation. *Energy Reports*, 6:165–171, February 2020. URL: https://www.sciencedirect.com/science/article/pii/S2352484719306845, doi:10.1016/j.egyr.2019.08.037.

[37] Florin Onea, Alexandra Diaconita, and Daniel Ganea. Assessment of the Black Sea High-Altitude Wind Energy. *Journal of Marine Science and Engineering*, 10:1463, October 2022. doi:10.3390/jmse10101463.

[38] Clara M. St. Martin, Julie K. Lundquist, Andrew Clifton, Gregory S. Poulos, and Scott J. Schreck. Wind turbine power production and annual energy production depend on atmospheric stability and turbulence. *Wind Energy Science*, 1(2):221–236, November 2016. Publisher: Copernicus GmbH. URL: https://wes.copernicus.org/articles/1/221/2016/, doi:10.5194/wes-1-221-2016.

[39] Fernando A. C. C. Fontes and Luís Tiago Paiva. Guaranteed collision avoidance in multi–kite power systems. 2017.

[40] Pietro Faggiani and Roland Schmehl. Design and economics of a pumping kite wind park. In Roland Schmehl, editor, *Airborne Wind Energy – Advances in Technology Development and Research*, Green Energy and Technology, chapter 16, pages 391–411. Springer, Singapore, 2018.

[41] M A Guerrero, E Romero, F Barrero, M I Milans, and E Gonzlez. Supercapacitors: Alternative Energy Storage Systems. 2009.

[42] Kashif Hussain, Mohd Salleh, Shi Cheng, and Yuhui Shi. Metaheuristic research: a comprehensive survey. *Artificial Intelligence Review*, 52, December 2019. doi:10.1007/s10462-017-9605-z.

[43] Ahmed Gad. Particle Swarm Optimization Algorithm and Its Applications: A Systematic Review. *Archives of Computational Methods in Engineering*, 29, April 2022. doi:10.1007/s11831-021-09694-4.

[44] Marco Dorigo and Thomas Stützle. *Ant colony optimization*. MIT Press, Cambridge, Mass, 2004.

[45] R.A. Rutenbar. Simulated annealing algorithms: an overview. *IEEE Circuits and Devices Magazine*, 5(1):19–26, January 1989. doi:10.1109/101.17235.

[46] Pradnya A. Vikhar. Evolutionary algorithms: A critical review and its future prospects. In *2016 International Conference on Global Trends in Signal Processing, Information Computing and Communication (ICGTSPICC)*, pages 261–265, December 2016.

[47] José Fernando Gonçalves and Mauricio G. C. Resende. Biased random-key genetic algorithms for combinatorial optimization. *Journal of Heuristics*, 17(5):487–525, October 2011.

[48] Leonardo de Almeida e Bueno. Biased random-key genetic algorithm for warehouse reshuffling. Publisher: Universidade Federal de Pernambuco, 2019.